KTH Engineering Sciences

Master of Science Thesis

Threshold Effects in SO(10) Grand Unified Theories

Erik Sönnerlind

Particle and Astroparticle Physics, Department of Physics,
School of Engineering Sciences,
KTH Royal Institute of Technology, SE-106 91 Stockholm, Sweden

Stockholm, Sweden 2020

Typeset in LaTeX

Examensarbete för avläggande av masterexamen i Teknisk Fysik, inom ämnesområdet teoretisk fysik.

Master's thesis for the degree of Master of Science, in the subject area of Theoretical Physics.

TRITA-SCI-GRU 2020:195

Abstract

In the field of theoretical particle physics, a major research direction is constructing theories that go beyond the Standard Model (SM) of particle physics. The SM is a very successful scientific theory, being able to describe and predict many observable phenomena. However, the SM suffers from several shortcomings, and it is evident that it is not sufficient as a final theory for describing the fundamental particles and their interactions. Some examples of its shortcomings are that it is not able to describe dark matter, neutrino masses, or the matter-antimatter asymmetry.

In this thesis, the issue at hand concerns some of the more aesthetic problems of the SM, namely that its gauge group, and the structure of the SM in general, can be regarded as rather ad hoc. One way of solving this is by having a Grand Unified Theory (GUT), where all of the SM gauge couplings unify into one at a high energy. Above that energy, the gauge group consists of only one simple factor, corresponding to one single interaction. Such theories can also provide descriptions for physics beyond the SM. One popular GUT gauge group is SO(10), which the models treated in this thesis will be based on. Specifically, two models will be discussed, where the difference is the intermediate symmetry group between SO(10) and the SM.

It has previously been shown that it is impossible to achieve unification in these two models at tree-level. However, when considering the matching between different gauge couplings at a higher order in perturbation theory, threshold effects must also be taken into account. We then investigate if this can save the two models. Many of the equations encountered are not possible to solve analytically, which is why a numerical analysis is a large part of the work performed in this thesis. As a result of that analysis, we find that it is possible to achieve unification in both of the investigated models. This comes at the cost of relatively large threshold corrections. We also find that taking into account the effects of kinetic mixing, in the model where it is possible, makes it easier to achieve unification among the gauge couplings.

Key words: Grand Unified Theory, renormalization group equations, threshold effects, kinetic mixing, gauge coupling unification.

Sammanfattning

Inom fältet teoretisk partikelfysik, så ligger mycket fokus på att skapa teorier som går bortom partikelfysikens standardmodell. Standardmodellen är en mycket framgångsrik vetenskaplig teori, som kan beskriva och förutspå många observerbara fenomen. Dock har standardmodellen ett antal problem, som gör det tydligt att den inte är tillräcklig som en slutgiltig teori för att beskriva fundamentalpartiklar och deras interaktioner. Några exempel på standardmodellens brister är att den inte kan beskriva mörk materia, neutrinomassor, eller asymmetrin mellan materia och antimateria.

I denna rapport ligger dock fokus på några mer estetiska problem med standardmodellen, nämligen att dess gaugegrupp, och modellens struktur i allmänhet, kan ses som en efterkonstruktion gjord för att passa observationer. Ett sätt att lösa detta är genom att ha en storförenad teori, där alla gaugekopplingar i standardmodellen förenas vid en hög energi. För energier över den föreningen finns det bara en gaugegruppsfaktor, och därför även bara en växelverkan. Sådana teorier kan även beskriva viss fysik bortom standardmodellen. En vanlig gaugegrupp för storförenade teorier är gruppen SO(10), vilken modellerna som behandlas här är baserade på. Två olika modeller kommer att undersökas, där skillnaden mellan de två är den mellanliggande symmetrigruppen mellan SO(10) och standardmodellen.

Det har visats tidigare att det är omöjligt att uppnå förening i båda dessa modeller vid lägsta ordningen i störningsräkning. När man undersöker matchningsvillkoren mellan olika gaugekopplingar vid en högre ordning, så måste man även ta hänsyn till tröskeleffekter. Vi undersöker då huruvida detta kan rädda de två modellerna. Många av ekvationerna som dyker upp här går inte att lösa analytiskt, vilket är varför en numerisk analys är en stor del av denna rapport. Vi ser från resultaten av den analysen att det är möjligt att uppnå förening i båda modellerna. Det kräver dock relativt höga tröskeleffekter. Vi finner också att inkludering av kinetisk blandning, i modellen där det är möjligt, gör det lättare att uppnå förening.

Nyckelord: Storförenad teori, renormeringsgruppsekvationer, tröskeleffekter, kinetisk blandning, gaugekopplingsförening.

Preface

Acknowledgements

First and foremost, I would like to thank my supervisor Tommy Ohlsson for having me as his student during the making of this thesis, and for his guidance and mentoring. Special thanks are also due to Marcus, for never getting tired of answering my questions, and for providing insight into life as a PhD student.

I would also like to thank Mattias for first answering questions about possible projects, as well as Sandhya and Monojit for coming up with other suggestions. I also want to thank all of the participants in the regularly held meetings, for interesting discussions and for sharing their experience in how to conduct research in theoretical particle physics. To them, as well as to the rest of the Particle and Astroparticle Physics group at KTH, I give thanks for contributing to the pleasant environment in the office, and for making it such a nice place to work.

Finally, my thanks go to family and friends who have supported me during the time I have been working on this thesis, and throughout my time at KTH.

Contents

Chapter 1

Introduction

Physics is about describing the world. In order to do this, we can create theories, which are mathematical models that describe a certain phenomenon. Valid physical theories can then be used to make predictions about outcomes of experiments. Particle physics deals with the very smallest constituents of what makes up the world around us, and how they interact with each other. In a sense, particle physics is therefore a field which is more fundamental than others.

Symmetries are an important part of the world, and in most areas of physics, symmetries play some part. One example of this is Noether's theorem, which relates symmetries to conserved quantities in classical and quantum mechanics. Some symmetries are easily seen in everyday life, such as translational or rotational symmetries, whereas other symmetries are more obscure. In either case, they are evident in the mathematical language used in physics. In theories of particle physics in particular, we are concerned with gauge symmetries, which are local transformations of the theory. These abstract symmetries are the very thing that generates the interactions between fundamental particles, by requiring that the theory remains gauge invariant, i.e. that the description of reality is not changed by removing redundant degrees of freedom in the mathematical model.

The best theory of particle physics that is available for us today is called the Standard Model (SM). It is a mathematical description of the fundamental particles that make up a large part of the Universe as we know it, including leptons, quarks, and scalar bosons. It also describes how these particles interact with each other, through the electromagnetic force, the weak force, and the strong force. These three forces are in turn mediated by different gauge bosons, which correspond to the gauge symmetries of the model. Over the years, the different particles described in the SM have been observed experimentally, which supports the underlying theory. The last piece of the puzzle that was required to complete the SM came in 2012, when the Higgs boson was discovered by the ATLAS and CMS collaborations at CERN [1, 2]. The SM is also highly successful when it comes to making accurate predictions of experimental results.

However, as beautiful as it may be, the SM still suffers from a number of significant shortcomings, as there are observed phenomena that cannot be described by the SM. First of all, the SM does not account for the effects of gravity, although such effects are disappearingly small when treating individual particles. The SM does also not provide a description for dark matter (DM), nor is it able to describe the matter–antimatter asymmetry observed in the Universe. It does also not include neutrino masses, and is therefore, by extension, not able to describe the neutrino oscillation phenomenon either. For example, neutrino oscillations were observed as early as 1998 [3].

There are also some aesthetic problems with the SM. What this means is that the structure of the SM can be considered ad hoc, in the sense that it is made to fit previous observations, instead of being based on some physical concepts. It also contains a number of parameters that need to be determined by fitting to experimental data. The values of these parameters cannot really be understood on a fundamental level. Although these shortcomings do not necessarily imply that the SM is wrong, they could be a sign that vital pieces of the puzzle are missing, and that the SM is only part of the picture—perhaps an effective theory only valid at lower energies.

As there are many reasons why the SM is not sufficient as the one and only theory of particle physics, new theories are needed that describe physics beyond the SM. One example of such an extended model is a Grand Unified Theory (GUT), where all of the gauge couplings unify at a high energy scale. This is possible, since the gauge couplings, i.e. the interaction strengths, of the theory become scale dependent as a result of renormalization. At the scale of unification, all three of the SM forces therefore merge into the same force. Not only would a GUT solve many of the aesthetic problems with the SM discussed earlier, but it would also accommodate new physics beyond the SM, such as providing a description of neutrino masses through the seesaw mechanism [4]. The first GUT based on a simple gauge group was proposed in 1974 [5], and had SU(5) as its gauge group. The investigation of GUTs then continued in the years to come [6], as new gauge groups and model structures were suggested.

The work performed in this thesis will focus on two different models, that both can be used in the creation of a GUT. Both models are based on having SO(10) as the unification gauge group. Such models are more complex than the original suggestions, but can also accommodate more physics. In these two models, it is not possible to achieve unification among the gauge couplings with tree-level matching conditions. However, so-called threshold effects appear when matching the couplings at a higher order in perturbation theory, which are a result of particles with masses around the symmetry breaking scales. Specifically, it will be investigated if threshold effects can save these two models, and thereby allowing unification.

1.1 Outline

This thesis is structured in the following way. In Ch. 2, we present necessary background theory for the project, including the SM, renormalization group running, and GUTs. Then, in Ch. 3, the two different models are presented, both based on SO(10) as a GUT gauge group, but with different intermediate symmetries. In Ch. 4, we discuss how these two models are affected by incorporating threshold effects. Finally, in Ch. 5, the numerical methods and results are presented, and in Ch. 6, we summarize and conclude the thesis.

Chapter 2

Background

This chapter will discuss some of the background theory that is relevant for the analysis performed in later chapters. It should by no means be considered as a complete description of the theoretical framework, but rather as a highlight of the most relevant areas, while also providing references to further reading. Theories based on gauge symmetries will be discussed, along with the gauge sector of the SM. Renormalization group running of coupling constants will then be explained, followed by an introduction to GUTs. The effects of kinetic mixing will also be included, as that is relevant for one of the models considered later. Then, threshold effects will be discussed, before we end the chapter with a discussion of proton decay.

2.1 Gauge theories

The theoretical framework of particle physics is mainly quantum field theories (QFTs), which incorporate special relativity, classical field theory, and quantum mechanics [7]. Therefore, they are equipped to deal with some of the highest energies and shortest distances that are available to us—making them the right tool for treating fundamental particles and their interactions. The foundation for any QFT is a Lagrangian density $\mathcal{L}$, often just called the Lagrangian of the theory. From this Lagrangian, written in terms of the fields of the theory, all other results can be derived.

A fundamental part of QFTs, and of physics in general, is symmetries. In particle physics, symmetries are operations that leave the Lagrangian invariant, and such operations can be seen as group elements. Of particular interest are symmetries that are local transformations of the fields, which means that the transformations themselves depend on the spacetime position x^μ. These are called gauge symmetries, and the groups that the operations are part of are called the gauge groups of the theory. Since gauge symmetries depend on the local coordinates, we will be

dealing with Lie groups, which are groups with elements that can be parametrized by continuous variables [8]. In a Lie group, a general element can be written as

$$g = \mathrm{e}^{\mathrm{i}\alpha^a T^a} \,. \tag{2.1}$$

Here, and henceforth, summation is implied over the group indices a. Also, α^a are the group parameters, and T^a denotes the generators of the group. Under a gauge transformation, a field ψ then transforms as

$$\psi \to \mathrm{e}^{\mathrm{i}\alpha^a T^a}\psi \,. \tag{2.2}$$

Different fields can transform under different representations of the gauge group, depending on the type of particle it describes.

That the Lagrangian remains gauge invariant is an important criterion. Together with the requirement of Lorentz invariance, it determines which terms are allowed in the Lagrangian, and which terms are not. Therefore, it has a large impact on the physics described by the theory. Let us consider a theory with a semi-simple gauge group

$$\mathcal{G} = G_1 \times G_2 \times \ldots \times G_n \,. \tag{2.3}$$

Some of these factors may be Abelian, meaning that their group elements commute, while some may be non-Abelian. For gauge invariance, we must introduce a gauge field for each of these factors. For an Abelian factor G_i we get a gauge field A^i_μ, whereas for a non-Abelian factor G_j we get a gauge field $A^{j,a}_\mu$. The difference is that the latter also has a group index a, taking the same number of different values as the number of generators in the group. For non-Abelian gauge theories, we use the Yang–Mills theory [9], which is the simplest example of a non-Abelian gauge theory. Gauge invariance then requires us to replace the derivative ∂_μ with the gauge covariant derivative

$$D_\mu = \partial_\mu - \mathrm{i}\sum_{i=1}^{n} g_i A^{i,a}_\mu T^{i,a} \,. \tag{2.4}$$

Here, g_i is the gauge coupling corresponding to the group factor G_i, $T^{i,a}$ is the properly normalized generators of that group, and $A^{i,a}_\mu$ is the corresponding gauge field. Note again that the group index a is only relevant for terms coming from non-Abelian factors. The kinetic terms containing other fields then result in interaction terms with the gauge bosons, since

$$\mathrm{i}\bar{\psi}\not{D}\psi = \ldots + \sum_{i=1}^{n} g_i A^{i,a}_\mu \bar{\psi}\gamma^\mu T^{i,a}\psi \,. \tag{2.5}$$

Thus, we see that interactions, or "forces", as they are often called, mediated by gauge bosons follow directly from requiring the Lagrangian to be gauge invariant.

Finally, we can then construct the gauge field strengths

$$F^{i,a}_{\mu\nu} = \partial_\mu A^{i,a}_\nu - \partial_\nu A^{i,a}_\mu + g_i f^{i,abc} A^{i,b}_\mu A^{i,c}_\nu \,, \tag{2.6}$$

where $f^{i,abc}$ are the structure constants of the gauge group factor G_i, given by

$$\left[T^{i,a}, T^{i,b}\right] = f^{i,abc} T^{i,c} \,. \tag{2.7}$$

Note that for an Abelian group, the structure constants vanish, since its generators commute. These gauge field strengths appear in the Lagrangian as gauge invariant terms on the form $F^{i,a}_{\mu\nu} F^{i,a,\mu\nu}$.

2.2 The Standard Model

The SM of particle physics is probably the most well-known QFT there is, as it is the theory for particle physics that is used today. There is a vast number of aspects that can be considered when discussing the SM, but the focus here will be on the gauge sector: the gauge groups, representations under those groups, and the resulting gauge interactions. The gauge group of the SM is

$$\mathcal{G}_{\text{SM}} = \text{SU}(3)_\text{C} \times \text{SU}(2)_\text{L} \times \text{U}(1)_Y \,. \tag{2.8}$$

The subscript of each group refers to the names of the charges, or quantum numbers, that they correspond to. The factor $\text{SU}(2)_\text{L} \times \text{U}(1)_Y$ is the gauge group for electroweak theory [10–12], describing weak and electromagnetic interactions. The label L refers to that only left-handed chiral particles are charged under $\text{SU}(2)_\text{L}$, while Y is the Abelian hypercharge. Furthermore, the $\text{SU}(3)_\text{C}$ factor is the gauge group for Quantum Chromodynamics (QCD) [13, 14], describing the strong interactions between quarks. The C therefore refers to the color charge of quarks.

Given the gauge group, we can also write down the gauge field strengths

$$\begin{aligned} G^a_{\mu\nu} &= \partial_\mu G^a_\nu - \partial_\nu G^a_\mu + g_{3\text{C}} f^{abc} G^b_\mu G^c_\nu \,, \\ W^a_{\mu\nu} &= \partial_\mu W^a_\nu - \partial_\nu W^a_\mu + g_{2\text{L}} \varepsilon^{abc} W^b_\mu W^c_\nu \,, \\ B_{\mu\nu} &= \partial_\mu B_\nu - \partial_\nu B_\mu \,, \end{aligned} \tag{2.9}$$

where G^a_μ, W^a_μ, and B_μ are the gauge fields for $\text{SU}(3)_\text{C}$, $\text{SU}(2)_\text{L}$, and $\text{U}(1)_Y$, respectively. Also, ε^{abc} are the structure constants of SU(2), which are the same as the elements of the Levi-Civita tensor. We can note that the gauge field corresponding to the Abelian group has no group index, while $a = 1, 2, 3$ for SU(2) and $a = 1, \ldots, 8$ for SU(3). The number of possible indices corresponds to the number of generators in the group, which for $\text{SU}(N)$ is $N^2 - 1$. The covariant derivative becomes

$$D_\mu = \partial_\mu - \text{i} g_{3\text{C}} G^a_\mu T^a - \text{i} g_{2\text{L}} W^b_\mu T^b - \text{i} g_{1Y} B_\mu Y \,, \tag{2.10}$$

where T^a in the second term denotes the generators of $\text{SU}(3)_\text{C}$, and T^b in the third term denotes the generators of $\text{SU}(2)_\text{L}$. Also, gauge fields transform as part of the

adjoint representation of each group, meaning that we have the three representations

$$(\mathbf{8},\mathbf{1})_0, \quad (\mathbf{1},\mathbf{3})_0, \quad (\mathbf{1},\mathbf{1})_0\,. \tag{2.11}$$

When writing representations like this, the first boldface number denotes the representation under $\mathrm{SU}(3)_\mathrm{C}$, the second one is the representation under $\mathrm{SU}(2)_\mathrm{L}$, and the subscript is the corresponding hypercharge value. The same convention will be used throughout this thesis, with boldface numbers denoting the dimension of representations under non-Abelian groups, and subscripts denoting charges under Abelian groups. Therefore, **8** and **3** in Eq. (2.11) are the adjoint representations of $\mathrm{SU}(3)_\mathrm{C}$ and $\mathrm{SU}(2)_\mathrm{L}$, respectively, since the dimensions of those are the same as the number of generators for each group. Also, **1** denotes the trivial representation, which means that the field in question is neutral under that particular group.

We are also interested in the other particle content of the SM, and how it transforms under the gauge group factors. The Weyl fermions have representations given by

$$\begin{aligned} &Q_L \sim (\mathbf{3},\mathbf{2})_{1/6}\,, \quad u_R \sim (\mathbf{3},\mathbf{1})_{2/3}\,, \quad d_R \sim (\mathbf{3},\mathbf{1})_{-1/3}\,, \\ &L_L \sim (\mathbf{1},\mathbf{2})_{-1/2}\,, \quad \ell_R \sim (\mathbf{1},\mathbf{1})_{-1}\,, \end{aligned} \tag{2.12}$$

where there are three generations of each field, and the subscripts L and R denote left- and right-handed fields, respectively. Also, in the scalar sector, we have the complex scalar Higgs, with a representation given by

$$\Phi \sim (\mathbf{1},\mathbf{2})_{1/2}\,. \tag{2.13}$$

The boldface numbers **2** and **3** now denote the fundamental representations of $\mathrm{SU}(2)_\mathrm{L}$ and $\mathrm{SU}(3)_\mathrm{C}$, respectively. This means that the fields are doublets or triplets under the corresponding group. The representation matrices of the generators in the fundamental representation of $\mathrm{SU}(2)_\mathrm{L}$ and $\mathrm{SU}(3)_\mathrm{C}$ are the three Pauli matrices, as well as the eight Gell-Mann matrices, normalized appropriately. This particle content then gives us the expected behavior—the left-handed quarks (Q_L) and leptons (L_L) as well as the complex Higgs (Φ) are the only ones being doublets under $\mathrm{SU}(2)_\mathrm{L}$, while all of the quarks (Q_L, u_R, d_R) are the only ones having color charge and transforming non-trivially under $\mathrm{SU}(3)_\mathrm{C}$. Also, the hypercharge assignments for each field give the correct electric charges after electroweak symmetry breaking.

2.2.1 The Higgs mechanism

When discussing the gauge structure of the SM, we must also mention the Higgs mechanism [15–18]. Not only is it a vital part of the SM and the physics it describes, but it also illustrates the concept of symmetry breaking in gauge theories—which is essential for the later analysis of the different models. Because of this, it can

be instructive to look at the details. In the SM, symmetry breaking occurs in the electroweak sector. What happens is that the electroweak gauge group is broken as

$$\mathrm{SU}(2)_\mathrm{L} \times \mathrm{U}(1)_Y \to \mathrm{U}(1)_Q \,, \tag{2.14}$$

by introducing a complex scalar Higgs field. As mentioned earlier, this field can be written as

$$\Phi = \begin{bmatrix} \phi^+ \\ \phi^0 \end{bmatrix} \sim (\mathbf{1}, \mathbf{2})_{1/2} \,, \tag{2.15}$$

which means that it is neutral under $\mathrm{SU}(3)_\mathrm{C}$, a doublet under $\mathrm{SU}(2)_\mathrm{L}$, and has hypercharge $\frac{1}{2}$. Minimizing the potential of this scalar field, given by

$$V(\Phi) = -\mu^2 \left(\Phi^\dagger \Phi\right) + \frac{\lambda}{4} \left(\Phi^\dagger \Phi\right)^2 \,, \tag{2.16}$$

we find that it takes a non-zero value in the vacuum, giving the vacuum expectation value (VEV)

$$\langle \Phi \rangle_0 = \langle 0 | \Phi | 0 \rangle = \begin{bmatrix} 0 \\ \sqrt{\frac{2\mu^2}{\lambda}} \end{bmatrix} \equiv \frac{1}{\sqrt{2}} \begin{bmatrix} 0 \\ v \end{bmatrix} . \tag{2.17}$$

This VEV breaks the previous symmetry of the vacuum, since now not all directions in that abstract space are equal. We can find the effects this has on the couplings and charges by looking at the kinetic term

$$\mathcal{L}_{\text{Higgs,kin}} = (D_\mu \Phi)^\dagger (D^\mu \Phi) \,, \tag{2.18}$$

in the Lagrangian of the scalar field. For this we need to take a closer look at the covariant derivative. There are four generators of the subgroup $\mathrm{SU}(2)_\mathrm{L} \times \mathrm{U}(1)_Y$ of $\mathcal{G}_\mathrm{SM}$, and four corresponding gauge fields. The covariant derivative then becomes

$$D_\mu = \partial_\mu - \mathrm{i} g_{1Y} Y B_\mu - \mathrm{i} g_{2\mathrm{L}} T^a W_\mu^a \,. \tag{2.19}$$

Expanding the Higgs field around the VEV in Eq. (2.17) then gives the term $(D_\mu \langle \Phi \rangle_0)^\dagger (D^\mu \langle \Phi \rangle_0)$ in the Lagrangian, which becomes a mass term for certain gauge bosons. To show this, we need that in the fundamental representation of $SU(2)$ we have $T^a = \frac{\sigma^a}{2}$, where σ^a are the Hermitian Pauli matrices

$$\sigma^1 = \begin{bmatrix} 0 & 1 \\ 1 & 0 \end{bmatrix}, \quad \sigma^2 = \begin{bmatrix} 0 & -\mathrm{i} \\ \mathrm{i} & 0 \end{bmatrix}, \quad \sigma^3 = \begin{bmatrix} 1 & 0 \\ 0 & -1 \end{bmatrix} . \tag{2.20}$$

Expanding the term containing the VEV, we then find that

$$\begin{aligned} (D_\mu \langle \Phi \rangle_0)^\dagger (D^\mu \langle \Phi \rangle_0) &= \langle \Phi \rangle_0^\dagger \left(\mathrm{i} g_{1Y} Y B_\mu + \frac{1}{2} \mathrm{i} g_{2\mathrm{L}} \sigma^a W_\mu^a \right) \\ &\quad \times \left(-\mathrm{i} g_{1Y} Y B^\mu - \frac{1}{2} \mathrm{i} g_{2\mathrm{L}} \sigma^a W^{a,\mu} \right) \langle \Phi \rangle_0 \\ &= \frac{v^2}{8} \left[\left(g_{1Y} B_\mu - g_{2\mathrm{L}} W_\mu^3 \right)^2 + g_{2\mathrm{L}}^2 \left((W_\mu^1)^2 + (W_\mu^2)^2 \right) \right] . \end{aligned} \tag{2.21}$$

This expression is not diagonal, which means that the actual mass eigenstates will be linear combinations of these gauge fields. We can rewrite the mass term as

$$(D_\mu \langle\Phi\rangle_0)^\dagger (D^\mu \langle\Phi\rangle_0) = \begin{bmatrix} W_\mu^1 & W_\mu^2 \end{bmatrix} M_W \begin{bmatrix} W^{1,\mu} \\ W^{2,\mu} \end{bmatrix} + \frac{1}{2} \begin{bmatrix} B_\mu & W_\mu^3 \end{bmatrix} M_G \begin{bmatrix} B^\mu \\ W^{3,\mu} \end{bmatrix}, \quad (2.22)$$

and we can find the mass states by diagonalizing the two mass matrices. We have

$$M_G = \frac{v^2}{4} \begin{bmatrix} g_{1Y}^2 & -g_{1Y} g_{2\mathrm{L}} \\ -g_{1Y} g_{2\mathrm{L}} & g_{2\mathrm{L}}^2 \end{bmatrix}, \quad (2.23)$$

which has one massless eigenstate ($m = 0$) given by

$$A_\mu = \frac{1}{\sqrt{g_{1Y}^2 + g_{2\mathrm{L}}^2}} \left(g_{2L} B_\mu + g_{1\mathrm{Y}} W_\mu^3 \right) . \quad (2.24)$$

This is the massless photon, which corresponds to the remaining unbroken symmetry $\mathrm{U}(1)_Q$. The other eigenstate of M_G is given by

$$Z_\mu^0 = \frac{1}{\sqrt{g_{1Y}^2 + g_{2\mathrm{L}}^2}} \left(g_{2\mathrm{L}} W_\mu^3 - g_{1Y} B_\mu \right) , \quad (2.25)$$

with a mass eigenvalue of $m_Z = \frac{v}{2}\sqrt{g_{1Y}^2 + g_{2\mathrm{L}}^2}$. This is the massive Z boson, which now has acquired a mass due to the symmetry breaking. The same thing happens to the two eigenstates of M_W, which are the two W bosons. An important result is the effect this has on the charges of the remaining unbroken symmetry, and the corresponding coupling constant. Using the previous expressions, we see that

$$\begin{aligned} \frac{1}{g_{1Y}} A_\mu - \frac{1}{g_{2\mathrm{L}}} Z_\mu^0 &= \frac{\sqrt{g_{1Y}^2 + g_{2\mathrm{L}}^2}}{g_{1Y} g_{2\mathrm{L}}} B_\mu , \\ \frac{1}{g_{2\mathrm{L}}} A_\mu + \frac{1}{g_{1Y}} Z_\mu^0 &= \frac{\sqrt{g_{1Y}^2 + g_{2\mathrm{L}}^2}}{g_{1Y} g_{2\mathrm{L}}} W_\mu^3 . \end{aligned} \quad (2.26)$$

Inserting into the covariant derivative in Eq. (2.19), and collecting all terms containing A_μ, we find that

$$D_\mu \supset -\mathrm{i} \frac{g_{1Y} g_{2\mathrm{L}}}{\sqrt{g_{1Y}^2 + g_{2\mathrm{L}}^2}} Y A_\mu - \mathrm{i} \frac{g_{1Y} g_{2\mathrm{L}}}{\sqrt{g_{1Y}^2 + g_{2\mathrm{L}}^2}} T^3 A_\mu = -\mathrm{i} \frac{g_{1Y} g_{2\mathrm{L}}}{\sqrt{g_{1Y}^2 + g_{2\mathrm{L}}^2}} (Y + T^3) A_\mu . \quad (2.27)$$

We can then identify the electric charge

$$Q = Y + T^3 , \quad (2.28)$$

as well as the coupling constant

$$g_{1Q} = \frac{g_{1Y} g_{2\mathrm{L}}}{\sqrt{g_{1Y}^2 + g_{2\mathrm{L}}^2}} . \quad (2.29)$$

This then finally gives that, at the scale of symmetry breaking, we have the matching condition

$$\alpha_{1Q}^{-1} \equiv \frac{4\pi}{g_{1Q}^2} = 4\pi \frac{g_{1Y}^2 + g_{2\mathrm{L}}^2}{g_{1Y}^2 g_{2\mathrm{L}}^2} = \frac{4\pi}{g_{1Y}^2} + \frac{4\pi}{g_{2\mathrm{L}}^2} \equiv \alpha_{1Y}^{-1} + \alpha_{2\mathrm{L}}^{-1} \,. \tag{2.30}$$

This kind of process happens many times during the evolution of the Universe, and in the following chapters; a scalar field acquires a VEV and breaks a symmetry, resulting in a matching condition between the couplings of the different groups.

2.3 Running of couplings

2.3.1 Renormalization

One major problem that arises in perturbation theory is that certain Feynman diagrams have infinite amplitudes, when considering diagrams up to a finite order. These infinities come from divergent spacetime integrals, stemming from the propagators running in loops in the diagrams. For example, a photon propagator with four-momentum k^μ running in a loop gives the factor

$$\int \frac{\mathrm{d}^4 k}{(4\pi)^2} \frac{1}{k^2 + \mathrm{i}\varepsilon} \,. \tag{2.31}$$

The first step in remedying this issue is finding a way of quantifying the divergencies of the problematic integrals, and thus enabling comparison of the severity of the divergencies of different integrals. This process is called regularization, and there are several different ways of going about it. One of the most useful approaches is known as dimensional regularization [19, 20], and is done by performing the calculations with a spacetime dimension of $d = 4 - \varepsilon$, and later letting $\varepsilon \to 0$ to retrieve the original result with four dimensions. It then turns out that these integrals can be rewritten on a few different forms with given results, an example of which is

$$\int \frac{\mathrm{d}^d l}{(2\pi)^d} \frac{1}{[l^2 - \Delta]^n} = \frac{(-1)^n \mathrm{i}}{(4\pi)^{d/2}} \frac{\Gamma\left(n - \frac{d}{2}\right)}{\Gamma(n)} \left(\frac{1}{\Delta}\right)^{n - \frac{d}{2}} \,. \tag{2.32}$$

Series expanding such expressions around the small parameter ε then for example gives

$$\frac{1}{(4\pi)^{d/2}} \Gamma\left(2 - \frac{d}{2}\right) \left(\frac{1}{\Delta}\right)^{2 - d/2} \approx \frac{1}{(4\pi)^2} \left(\frac{2}{\varepsilon} - \gamma - \log(\Delta) + \log(4\pi)\right) \,, \tag{2.33}$$

and the divergent terms can be identified as those that diverge when $\varepsilon \to 0$. Here, γ denotes the Euler–Mascheroni constant. Another notable way of regularizing

divergent integrals is the Pauli–Villars regularization prescription [21], which is based on modifying the propagators as

$$\frac{1}{k^2+\mathrm{i}\varepsilon} \to \frac{1}{k^2+\mathrm{i}\varepsilon} - \frac{1}{k^2-\Lambda^2+\mathrm{i}\varepsilon}\,. \tag{2.34}$$

Here, Λ is a parameter that is inserted to measure how the integral diverges, just like ε in the previous case. The original result is then retrieved in the limit $\Lambda \to \infty$. Such a parameter can also be introduced as a cutoff for the integration limit in the divergent integrals [7], thereby making the change

$$\int_0^\infty \mathrm{d}k \to \int_0^\Lambda \mathrm{d}k\,. \tag{2.35}$$

The same limit as earlier, i.e. $\Lambda \to \infty$, is then taken to check the divergency.

Having a measure of how badly the different integrals diverge then allows us to renormalize the theory, in order to remove the divergencies. This is done by rescaling the fields, masses, and coupling constants in the Lagrangian. Doing that relates the bare quantities in the original Lagrangian to the physical ones, which are actually measured in experiments. By doing this we can then separate the Lagrangian as

$$\mathcal{L} = \mathcal{L}_0 + \delta\mathcal{L}\,, \tag{2.36}$$

where $\mathcal{L}_0$ contains the physical quantities, and $\delta\mathcal{L}$ contains the so-called counterterms. The important part is that these counterterms remove all of the divergencies from the physical part. In the minimal subtraction scheme [22, 23], the divergent part, and nothing else, is absorbed by the counterterms. However, in other renormalization schemes, we can also choose to remove superfluous constants along with the divergent terms. For example, in commonly used modified minimal subtraction scheme, the extra constants appearing in Eq. (2.33) are removed as well.

A key point is that regularizing divergent integrals and renormalizing the theory introduces a dependence on the energy scale μ, also called the renormalization scale, for the physical parameters in the theory that appear in $\mathcal{L}_0$. What is of interest to us is the so-called β-function, which describes the scale dependence of the coupling constants. The relation is given by the differential equation

$$\frac{\mathrm{d}g_i}{\mathrm{d}\log(\mu)} = \beta_i(g_1, g_2, \ldots, g_n)\,. \tag{2.37}$$

The β-function on the right-hand side can be calculated from the counterterms appearing in the renormalized theory, and can therefore be calculated to different orders in perturbation theory, corresponding to how many loops are allowed in those diagrams.

2.3.2 One-loop order

For the time being, we will assume that no more than one of the factors in the gauge group is Abelian. If there are several Abelian group factors, a phenomenon called

kinetic mixing can be taken into account [24]. This will be discussed in section 2.5. To one-loop order, the β-function for the coupling g_i becomes

$$\beta_i(g_1, g_2, \ldots, g_n) = \frac{b_i}{16\pi^2} g_i^3 \,, \tag{2.38}$$

and is therefore only a function of that specific coupling. The coefficient b_i is given by

$$b_i = -\frac{1}{3}\left[11C_2\left(G_i\right) - 4\kappa_F C(F_i) - \kappa_S C(S_i)\right] \,. \tag{2.39}$$

In the following parts, we will let T_r^a denote the representation matrices of group generators T_a in the representation r, where a again is the group index running from 1 to the total number of generators of the group. In Eq. (2.39), $C(r)$ is a group invariant sometimes called the Dynkin index, defined by

$$\mathrm{Tr}\left[T_r^a, T_r^b\right] = C(r)\delta^{ab}. \tag{2.40}$$

Also, $C_2(G_i)$ is the quadratic Casimir in the adjoint representation of the group G_i (denoted by $r = G_i$), given by

$$T_{G_i}^a T_{G_i}^a = C_2(G_i) I \,, \tag{2.41}$$

where a sum over the group indices is implied and the identity matrix I acts on the same space as the representation matrices. These two invariants are related by

$$C(r) = \frac{d(r)}{d(G)} C_2(r) \,, \tag{2.42}$$

where $d(r)$ is the dimension of the representation r, and $d(G)$ is the dimension of the adjoint representation [8]. The dimension of a group representation is the dimension of the space that the representation matrices act on (e.g. $d(r) = 3$ if T_r^a are 3×3 matrices). In Eq. (2.39), it is also implied that the last two terms contain a sum over all the particle content in the theory, where F_i denotes the fermion representations under the group G_i, and S_i denotes the scalar representations under that same group. Then, for each such term, κ_F is 1 for Dirac fermions and 1/2 for Weyl fermions, and κ_S is 1 for complex scalars and 1/2 for real scalars. It can be noted that $C(r) = 0$ for the trivial representation, meaning that only fields transforming non-trivially under the group G_i contribute to the running of the corresponding coupling constant.

Because of this relatively simple form of the β-function at one-loop order, it is possible to solve the equation analytically for each of the coupling constants. If

we let a dot denote a derivative with respect to $\log(\mu)$, the differential equation becomes

$$\dot{g}_i = \frac{b_i}{16\pi^2} g_i^3 \,, \tag{2.43}$$

which is separable, since it can be written as

$$\frac{\dot{g}_i}{g_i^3} = \frac{b_i}{16\pi^2} \,. \tag{2.44}$$

Integrating, we find that

$$-\frac{1}{2}\frac{1}{g_i^2} = \frac{b_i}{16\pi^2}\log(\mu) + C \,, \tag{2.45}$$

where C is an integration constant. Usually, what we are interested in is actually α_i^{-1}, where $\alpha_i = \frac{g_i^2}{4\pi}$, which means that this form is useful. Also, initial values are often given by experimental data at $\mu = M_{\mathrm{Z}}$, where $M_{\mathrm{Z}} \approx 91.1876\,\mathrm{GeV}$ is the mass of the Z boson. This means that we end up with expressions on the form

$$\alpha_i^{-1}(\mu) = -\frac{b_i}{2\pi}\log\left(\frac{\mu}{M_{\mathrm{Z}}}\right) + \alpha_i^{-1}(M_{\mathrm{Z}}) \,. \tag{2.46}$$

Of course, if the initial values are given at some other energy scale, M_{Z} can just be exchanged for that scale.

2.3.3 Two-loop order

The β-function can also be calculated to two-loop order, which makes things considerably more complicated. It is now given by

$$\beta_i(g_1, g_2, \ldots, g_n) = \frac{b_i}{16\pi^2} g_i^3 + \sum_j \frac{B_{ij}}{(16\pi^2)^2} g_i^3 g_j^2 \,, \tag{2.47}$$

where the sum runs over all the group factors $j = 1, 2, \ldots, n$. This means that in general, the β-function for the coupling g_i is no longer a function of only that coupling, and the system of n differential equations instead becomes coupled. The two-loop coefficients in front of the mixed terms have been calculated previously in different cases [25–29], and can be neatly expressed as [30]

$$\begin{aligned} B_{ij} = &-\frac{34}{3}\left[C_2(G_i)\right]^2 \delta_{ij} + \kappa_F \left[4C_2(F_j) + \frac{20}{3}C_2(G_i)\delta_{ij}\right] C(F_i) \\ &+ \kappa_S \left[4C_2(S_j) + \frac{2}{3}C_2(G_i)\delta_{ij}\right] C(S_i) \,, \end{aligned} \tag{2.48}$$

where the notation for the group coefficients is the same as in the one-loop case, and the sum over all particle content is implied in the same way. The differential

equation in Eq. (2.37) can no longer be solved analytically, and we now must resort to numerical methods. For this purpose, it can be useful to rewrite the equation in terms of α_i^{-1}, instead of g_i. We get

$$\frac{\mathrm{d}\alpha_i^{-1}}{\mathrm{d}\log(\mu)} = \frac{\mathrm{d}}{\mathrm{d}\log(\mu)}\left(\frac{4\pi}{g^2}\right) = -\frac{b_i}{2\pi} - \sum_j \frac{B_{ij}}{8\pi^2\alpha_j^{-1}}\,, \tag{2.49}$$

where we again used that $g_j^2 = 4\pi/\alpha_j^{-1}$. Finally, we can rewrite this equation as to use derivatives with respect to μ, instead of with respect to $\log(\mu)$, which might be useful in certain numerical scenarios. The chain rule gives

$$\frac{\mathrm{d}\alpha_i^{-1}}{\mathrm{d}\log(\mu)} = \left(\frac{\mathrm{d}\log(\mu)}{\mathrm{d}\mu}\right)^{-1}\frac{\mathrm{d}\alpha_i^{-1}}{\mathrm{d}\mu} = \mu\frac{\mathrm{d}\alpha_i^{-1}}{\mathrm{d}\mu}\,, \tag{2.50}$$

which then gives

$$\frac{\mathrm{d}\alpha_i^{-1}}{\mathrm{d}\mu} = -\frac{b_i}{2\pi\mu} - \sum_j \frac{B_{ij}}{8\pi^2\alpha_j^{-1}\mu}\,. \tag{2.51}$$

2.3.4 Running in the Standard Model

Let us then look at the running of the coupling constants in the SM, where the gauge group is

$$\mathcal{G}_{\mathrm{SM}} = \mathrm{SU}(3)_{\mathrm{C}} \times \mathrm{SU}(2)_{\mathrm{L}} \times \mathrm{U}(1)_Y\,. \tag{2.52}$$

Given how the particle content transforms under the gauge group, we can use the expressions in Eqs. (2.39) and (2.48) to list the β-function coefficients to both orders in perturbation theory. To one-loop order, we get

$$b = \begin{bmatrix} b_{1Y} & b_{2\mathrm{L}} & b_{3\mathrm{C}} \end{bmatrix} = \begin{bmatrix} \frac{41}{10} & -\frac{19}{6} & -7 \end{bmatrix}, \tag{2.53}$$

where the indices $1Y$, 2L, and 3C again correspond to $\mathrm{U}(1)_Y$, $\mathrm{SU}(2)_{\mathrm{L}}$, and $\mathrm{SU}(3)_{\mathrm{C}}$, respectively. Inserting in Eq. (2.46), we then get the analytical solutions

$$\begin{aligned} \alpha_{1Y}^{-1} &= -\frac{41}{20\pi}\log\left(\frac{\mu}{M_{\mathrm{Z}}}\right) + \alpha_{1Y}^{-1}(M_{\mathrm{Z}})\,, \\ \alpha_{2\mathrm{L}}^{-1} &= \frac{19}{12\pi}\log\left(\frac{\mu}{M_{\mathrm{Z}}}\right) + \alpha_{2\mathrm{L}}^{-1}(M_{\mathrm{Z}})\,, \\ \alpha_{3\mathrm{C}}^{-1} &= \frac{7}{2\pi}\log\left(\frac{\mu}{M_{\mathrm{Z}}}\right) + \alpha_{3\mathrm{C}}^{-1}(M_{\mathrm{Z}})\,, \end{aligned} \tag{2.54}$$

which describe the running of the coupling constants at one-loop order. In a similar way, we get to two-loop order

$$B = \begin{bmatrix} B_{1Y,1Y} & B_{1Y,2\mathrm{L}} & B_{1Y,3\mathrm{C}} \\ B_{2\mathrm{L},1Y} & B_{2\mathrm{L},2\mathrm{L}} & B_{2\mathrm{L},3\mathrm{C}} \\ B_{3\mathrm{C},1Y} & B_{3\mathrm{C},2\mathrm{L}} & B_{3\mathrm{C},3\mathrm{C}} \end{bmatrix} = \begin{bmatrix} \frac{199}{50} & \frac{27}{10} & \frac{44}{5} \\ \frac{9}{10} & \frac{35}{6} & 12 \\ \frac{11}{10} & \frac{9}{2} & -26 \end{bmatrix}. \tag{2.55}$$

As mentioned earlier, this leads to three coupled differential equations that must be solved numerically. When solving them, as well as when plotting the exact one-loop solutions, initial values based on data from the Particle Data Group [31] are used. The values used here are given by

$$\begin{aligned} \alpha_{1Y}^{-1}(M_Z) &= 59.011\,, \\ \alpha_{2L}^{-1}(M_Z) &= 29.586\,, \\ \alpha_{3C}^{-1}(M_Z) &= 8.503\,. \end{aligned} \tag{2.56}$$

Figure 2.1 shows a plot of α_i^{-1} for the three different couplings, as functions of μ, with a logarithmic horizontal axis. The one-loop order running is plotted directly from the analytical expressions, while the two-loop results are plotted using a numerical differential equation solver. We then see that in this case, the corrections added by the two-loop order terms make a relatively small impact.

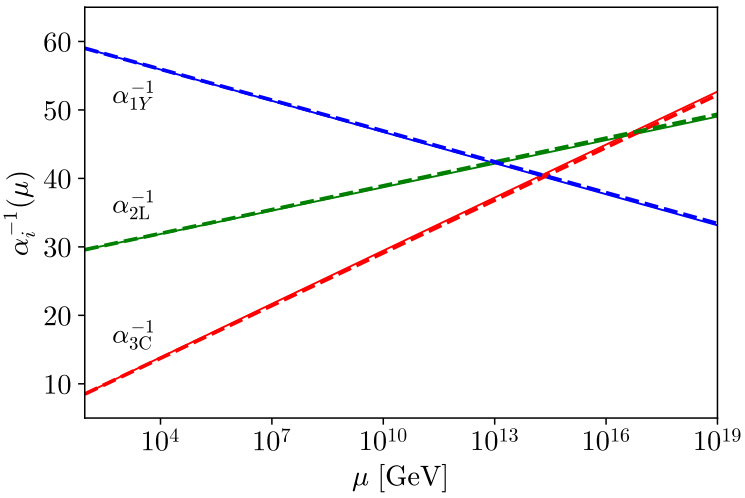

Figure 2.1: The running of the three gauge couplings in the SM, to one-loop order (dashed) and two-loop order (solid).

2.4 Grand Unified Theories

One major aesthetic issue with the SM is the question of why the gauge group consists of the three particular factors in Eq. (2.8), and what motivates the seemingly unwarranted difference in coupling strength between the different interactions. Many suggested extensions of the SM are therefore GUTs. In a GUT, the gauge couplings unify at some high energy scale, above which the gauge group only has one single factor, and therefore also only one gauge coupling. Through symmetry

breaking, this unified gauge group is broken down to the SM factors at lower energies, which is what we are able to observe in experiments. From the plot in figure 2.1, it is evident that such unification does not occur in the SM, and therefore also that something more needs to be added to the model.

2.4.1 Grand Unification gauge groups

SU(5)

One of the simplest candidates for having a single simple group as the gauge group is the group SU(5), which was first proposed in 1974 [5]. We can examine how the particle content transforms under this group, in order to reproduce the correct SM particle content at lower scales. The fermions are embedded in this group as [32]

$$\mathbf{10} \oplus \overline{\mathbf{5}}\,, \tag{2.57}$$

where the boldface number is the dimension of the representation of the field under SU(5). To see how the SM fermions are ordered in these multiplets, we can observe how these representations are broken down into $\mathcal{G}_{\mathrm{SM}}$. We get

$$\begin{aligned} \mathbf{10} &\to (\overline{\mathbf{3}}, \mathbf{1})_{-2/3} \oplus (\mathbf{3}, \mathbf{2})_{1/6} \oplus (\mathbf{1}, \mathbf{1})_{1} = u_R^c \oplus Q_L \oplus \ell_R^c\,, \\ \overline{\mathbf{5}} &\to (\overline{\mathbf{3}}, \mathbf{1})_{1/3} \oplus (\mathbf{1}, \mathbf{2})_{-1/2} = d_R^c \oplus L_L\,, \end{aligned} \tag{2.58}$$

where we used our knowledge of the SM representations from earlier, to see how the SM fermions fit into these larger representations. Also, the superscript c denotes charge conjugation. Finally, there are scalars in the representations

$$\mathbf{5}_{\mathrm{H}} \oplus \mathbf{24}_{\mathrm{H}}\,, \tag{2.59}$$

while the gauge bosons are in the adjoint **24**. The subscript H here just points out the fact that these are representations of scalar fields, which can be seen as generalized Higgses. They are chosen in the easiest way that still reproduces the correct SM content. Specifically, the $\mathbf{24}_{\mathrm{H}}$ is the representation that acquires a VEV at some scale in order to break SU(5) to $\mathcal{G}_{\mathrm{SM}}$, while $\mathbf{5}_{\mathrm{H}}$ is needed to reproduce the SM Higgs, which in turn is needed for electroweak symmetry breaking. The latter follows from

$$\mathbf{5}_{\mathrm{H}} \to (\mathbf{3}, \mathbf{1})_{-1/3} \oplus (\mathbf{1}, \mathbf{2})_{1/2} = (\mathbf{3}, \mathbf{1})_{-1/3} \oplus \Phi\,. \tag{2.60}$$

As we can see, this also produces an extra scalar in the representation $(\mathbf{3}, \mathbf{1})_{-1/3}$, which is an SU(3) triplet. Since this is not part of the SM, we can let that field have a very large mass, in order to prevent it from affecting physics at low scales.

SO(10)

Another candidate of a simple gauge group for grand unification is SO(10) [33–37]. In a model with this gauge group, the fermions can be embedded in a single 16-dimensional irreducible representation $\mathbf{16}_{\mathrm{F}}$, where we now use the subscript F to

label the fermion representation. This can be seen from that when breaking SO(10) into $\mathcal{G}_{\mathrm{SM}}$, we get

$$\begin{aligned}\mathbf{16}_{\mathrm{F}} &\to (\mathbf{3},\mathbf{2})_{1/6} \oplus (\mathbf{1},\mathbf{2})_{-1/2} \oplus (\overline{\mathbf{3}},\mathbf{1})_{1/3} \oplus (\overline{\mathbf{3}},\mathbf{1})_{-2/3} \oplus (\mathbf{1},\mathbf{1})_{1} \oplus (\mathbf{1},\mathbf{1})_{0} \\ &= Q_L \oplus L_L \oplus d_R^c \oplus u_R^c \oplus \ell_R^c \oplus (\mathbf{1},\mathbf{1})_0 \,.\end{aligned} \tag{2.61}$$

Therefore, this single representation yields all SM fermions, which is a very compelling argument for this gauge group. We also get an extra representation $(\mathbf{1},\mathbf{1})_0$, which is completely neutral under the SM. This can just be seen as the missing right-handed neutrino, which has not been observed interacting with the SM. Furthermore, the gauge bosons again reside in the adjoint representation **45** of SO(10). Now, there are also different possible scalars that all reproduce the SM Higgs, for example $\mathbf{10}_{\mathrm{H}}$, $\overline{\mathbf{126}}_{\mathrm{H}}$, or $\mathbf{120}_{\mathrm{H}}$.

However, directly breaking SO(10) to $\mathcal{G}_{\mathrm{SM}}$ is not the only way of creating a GUT based on this group. Since SO(10) is a group of rank 5, while $\mathcal{G}_{\mathrm{SM}}$ is a group of rank 4, there are many different ways of breaking the GUT gauge group down to the SM gauge group. Specifically, SO(10) can be broken to an intermediate symmetry, which in turn can be broken to $\mathcal{G}_{\mathrm{SM}}$ at an even lower scale. Which breaking chain is used significantly changes the behavior of the couplings at different energies, as both the matching conditions and the β-functions change. A summary of the different possible breaking chains is given in Ref. [37]. Such breaking chains are also the foundation of the different models that will be treated in this thesis.

2.4.2 Normalization of Abelian charges

When embedding the SM into a larger unified gauge group, one has to consider the appropriate normalization of the hypercharge Y that should be used [38]. Being the generator of the Abelian group $\mathrm{U}(1)_Y$, the normalization of Y can be chosen quite arbitrarily when considering the SM alone. However, the generators of other larger groups, such as $\mathrm{SU}(N)$ or $\mathrm{SO}(N)$, must be normalized in specific ways, in order to satisfy

$$\mathrm{Tr}\big[T_r^a T_r^b\big] = C(r)\delta^{ab} \,. \tag{2.62}$$

Here, $C(r)$ again denotes the Dynkin index of the representation denoted by r.

SU(5)

Let us first consider the case of having $\mathrm{SU}(5)$ as the simple gauge group at high energies. There are then 24 generators T^a of that group, each represented by a $n \times n$ matrix in a n-dimensional representation. However, one of these generators corresponds to the the $\mathrm{U}(1)_Y$ generator, three correspond to the three $\mathrm{SU}(2)_{\mathrm{L}}$ generators, and eight correspond to the eight $\mathrm{SU}(3)_{\mathrm{C}}$ generators of the subgroup

$\mathcal{G}_{\rm SM}$. There are two possible fermion representations we can look at. First of all, let us look at a field in the fundamental representation, where, as we saw earlier,

$$\overline{\mathbf{5}} \to (\overline{\mathbf{3}}, \mathbf{1})_{1/3} \oplus (\mathbf{1}, \mathbf{2})_{-1/2} = d_R^c \oplus L_L \,. \tag{2.63}$$

One such 5-plet therefore contains the right-handed down quark triplet, as well as the left-handed lepton doublet. From the SM charge assignments shown earlier, we then see that the hypercharge Y in this representation would become

$$Y = \text{diag}\left(\frac{1}{3}, \frac{1}{3}, \frac{1}{3}, -\frac{1}{2}, -\frac{1}{2}\right) , \tag{2.64}$$

giving

$$\text{Tr}\big[Y^2\big] = \frac{5}{6} \,. \tag{2.65}$$

Now, if we let the SU(5) generator T^i be the one corresponding to hypercharge, the normalization condition in Eq. (2.62) requires that

$$\text{Tr}\big[(T^i)^2\big] = C(\overline{\mathbf{5}}) = \frac{1}{2} \,. \tag{2.66}$$

Inserting a normalization factor so that $T^i = kY$ then gives

$$\frac{1}{2} = k^2 \,\text{Tr}\big[Y^2\big] = \frac{5}{6} k^2 \quad \Longrightarrow \quad k = \sqrt{\frac{3}{5}} \,. \tag{2.67}$$

We can also look at the fermions embedded in the 10-dimensional representation **10**. Hopefully, this will result in the same hypercharge normalization. In this representation, we saw earlier that

$$\mathbf{10} \to (\overline{\mathbf{3}}, \mathbf{1})_{-2/3} \oplus (\mathbf{3}, \mathbf{2})_{1/6} \oplus (\mathbf{1}, \mathbf{1})_1 = u_R^c \oplus Q_L \oplus \ell_R^c \,, \tag{2.68}$$

and as a result, we have

$$Y = \text{diag}\left(-\frac{2}{3}, -\frac{2}{3}, -\frac{2}{3}, \frac{1}{6}, \frac{1}{6}, \frac{1}{6}, \frac{1}{6}, \frac{1}{6}, \frac{1}{6}, 1\right) , \tag{2.69}$$

which then gives

$$\text{Tr}\big[Y^2\big] = \frac{5}{2} \,. \tag{2.70}$$

However, the normalization condition (2.62) now instead becomes

$$\text{Tr}\big[(T^i)^2\big] = C(\mathbf{10}) = \frac{3}{2} \,. \tag{2.71}$$

Again inserting a normalization factor for the hypercharge then gives

$$\frac{3}{2} = k^2 \,\text{Tr}\big[Y^2\big] = \frac{5}{2} k^2 \quad \Longrightarrow \quad k = \sqrt{\frac{3}{5}} \,. \tag{2.72}$$

We therefore get the same hypercharge normalization, no matter which representation we choose to look at. This normalization also affects the gauge couplings of the theory, since the covariant derivative then becomes

$$D_\mu = \partial_\mu - \mathrm{i}g_{1\mathrm{Y,SM}} Y B_\mu - \ldots = \partial_\mu - \mathrm{i}g_{1\mathrm{Y,GUT}} T^i B_\mu - \ldots \,, \tag{2.73}$$

where we left out the terms from the other gauge group factors. Here, B_μ is the gauge field from $\mathrm{U}(1)_Y$. In order to preserve this covariant derivative when exchanging Y for T^i, we must then change the coupling in the opposite way, giving

$$g_{1\mathrm{Y,GUT}} = \sqrt{\frac{5}{3}} g_{1\mathrm{Y,SM}} \,. \tag{2.74}$$

Since $\alpha_i = \frac{g_i^2}{4\pi}$, this then also leads to

$$\alpha_{1\mathrm{Y,GUT}}^{-1} = \frac{3}{5} \alpha_{1\mathrm{Y,SM}}^{-1} \,. \tag{2.75}$$

SO(10)

The same kind of normalization must be done for the unification gauge group that is most relevant in this work, which is SO(10). This group, which is of higher rank, instead has 45 different generators T^a. These generators also need to be normalized. All of the SM fermions in a generation (including even a right-handed neutrino) can under this group be embedded into a single 16-dimensional representation $\mathbf{16}_\mathrm{F}$, which means that we get

$$\mathrm{Tr}\big[Y^2\big] = 6\left(\frac{1}{6}\right)^2 + 3\left(\frac{2}{3}\right)^2 + 3\left(-\frac{1}{3}\right)^2 + 2\left(-\frac{1}{2}\right)^2 + (-1)^2 = \frac{10}{3} \,. \tag{2.76}$$

This result is independent of exactly how the different fields are ordered in the 16-plet, as it only depends on the number of times each value of Y appears. Comparing this with the generator T^i of SO(10) corresponding to $\mathrm{U}(1)_Y$, which according to Eq. (2.62) needs to satisfy

$$\mathrm{Tr}\big[(T^i)^2\big] = C(\mathbf{16}) = 2 \,, \tag{2.77}$$

we can again insert a factor k so that $T^i = kY$. We then find that

$$2 = k^2 \,\mathrm{Tr}\big[Y^2\big] = \frac{10}{3} k^2 \quad \Longrightarrow \quad k = \sqrt{\frac{3}{5}} \,. \tag{2.78}$$

Interestingly enough, we end up with exactly the same hypercharge normalization as we did when embedding the SM in SU(5). Thus, we again get

$$g_{1Y,\mathrm{GUT}} = \sqrt{\frac{5}{3}} g_{1Y,\mathrm{SM}} \,. \tag{2.79}$$

This normalization of the coupling constant was used throughout the previous part, when calculating the running in the SM. It is usually just referred to as the GUT

normalization of hypercharge, as it appears when considering both of these GUT gauge groups.

2.5 Kinetic mixing

As mentioned earlier, the case where there is more than one Abelian factor in the gauge group requires special attention. The reason for this is gauge invariance, which, as mentioned earlier, often is the determining factor in which terms are allowed in the Lagrangian. For a non-Abelian group, the corresponding field strength tensor $F^{a,\mu\nu}$ is not gauge invariant by itself. Therefore, we need terms such as $F^{a,\mu\nu}F^a_{\mu\nu}$, which appear in the gauge portion of the Lagrangian. However, for an Abelian group, $F^{\mu\nu}$ is gauge invariant by itself [39]. As long as there is only one Abelian factor, as is the case in the SM, this does not make a difference. Consider instead the case of a gauge group on the form

$$\mathcal{G} = \mathcal{G}_0 \times \mathrm{U}(1)_1 \times \ldots \times \mathrm{U}(1)_N, \tag{2.80}$$

which has N different Abelian factors, and $\mathcal{G}_0$ only contains non-Abelian factors. Let also $F^{i,\mu\nu}$, $i = 1, \ldots, N$, denote the field strength tensors corresponding to these different Abelian groups. The point is that now terms on the form $F^{i,\mu\nu}F^j_{\mu\nu}$, even when $i \neq j$, are both gauge invariant and Lorentz invariant, and can therefore appear in the Lagrangian. In general [40, 41], the kinetic gauge terms in the Lagrangian are on the form

$$\mathcal{L}_{\text{gauge,kin}} = F^{i,\mu\nu}\xi_{ij}F^j_{\mu\nu}\,, \tag{2.81}$$

where the symmetric matrix ξ no longer is the identity, or even necessarily diagonal. This is what constitutes the mixing; gauge bosons corresponding to different Abelian gauge groups become coupled to each other, with coupling strengths given by the off-diagonal elements in the matrix. Since a real $N \times N$ symmetric matrix contains $\frac{1}{2}N(N+1)$ free parameters, this means that $\frac{1}{2}N(N-1)$ new parameters are introduced into the model.

We now have possible Feynman diagrams[1] on the form

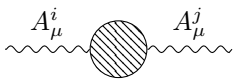

(2.82)

where $i \neq j$, and the blob can be a result of the mixing term, or fermions that are charged under both $\mathrm{U}(1)_i$ and $\mathrm{U}(1)_j$ simultaneously. Consequently, this kind of diagram gives rise to an effective interaction between a particle that is only charged under one of the two groups, and a particle that is only charged under the other one.

[1] This Feynman diagram, and all following ones, are created using the TikZ-Feynman package, from Ref. [42].

Thus, a field having a certain charge under one of the Abelian groups automatically implies some effective charge under the other Abelian groups. For the purpose of this work, the important implication of this is that it changes the β-functions, as more diagrams need to be considered during the renormalization process. Fortunately, the β-functions up to two-loop order have been calculated previously [43, 44]. What happens is that the β-functions seen earlier become extended with extra terms depending on the off-diagonal elements in ξ, which sometimes are called kinetic mixing coefficients. We can write this as

$$\beta(g_i) = \beta_0(g_i) + \beta_k(g_i)\,, \tag{2.83}$$

where $\beta_0(g_i)$ are the β-functions from section 2.3, where there is no kinetic mixing, and $\beta_k(g_i)$ is the additional contribution coming from taking mixing into account. For convenience, we only write out the coupling g_i as the argument, and use that as a label for the function, even though the β-function can depend on the other couplings as well.

2.5.1 Two-group mixing

Let us now look in more detail at the case where there are two Abelian factors in the gauge group, $\mathrm{U}(1)_1$ and $\mathrm{U}(1)_2$. This is the case that will be relevant for one of the models later. The kinetic gauge term for these two groups becomes

$$\begin{aligned}\mathcal{L}_{\text{gauge,kin}} &= -\frac{1}{4}F^{1,\mu\nu}F^1_{\mu\nu} - \frac{1}{4}F^{2,\mu\nu}F^2_{\mu\nu} - \frac{\chi}{2}F^{1,\mu\nu}F^2_{\mu\nu} \\ &= -\frac{1}{4}\begin{bmatrix}F^{1,\mu\nu} & F^{2,\mu\nu}\end{bmatrix}\begin{bmatrix}1 & \chi \\ \chi & 1\end{bmatrix}\begin{bmatrix}F^1_{\mu\nu} \\ F^2_{\mu\nu}\end{bmatrix},\end{aligned} \tag{2.84}$$

where χ is the mixing parameter. This expression is essentially a quadratic form, and can therefore be diagonalized by changing the gauge boson basis according to

$$\begin{bmatrix}A^1_\mu \\ A^2_\mu\end{bmatrix} = \frac{1}{\sqrt{2}}\begin{bmatrix}\frac{1}{\sqrt{1-\chi}} & -\frac{1}{\sqrt{1+\chi}} \\ \frac{1}{\sqrt{1-\chi}} & \frac{1}{\sqrt{1+\chi}}\end{bmatrix}\begin{bmatrix}B^1_\mu \\ B^2_\mu\end{bmatrix} = R\begin{bmatrix}B^1_\mu \\ B^2_\mu\end{bmatrix}, \tag{2.85}$$

where R denotes the given matrix containing the properly normalized eigenvectors of the matrix in Eq. (2.84). That expression now becomes

$$\mathcal{L}_{\text{gauge,kin}} = -\frac{1}{4}F'^{1,\mu\nu}F'^1_{\mu\nu} - \frac{1}{4}F'^{2,\mu\nu}F'^2_{\mu\nu}\,, \tag{2.86}$$

where the primes denote that we have moved to a different basis. By diagonalizing this expression, we have in a sense removed the mixing by finding the physical gauge bosons.

However, this does not completely remove the effects of kinetic mixing. What we now must look at is how the covariant derivative has changed, since that is what gives rise to interaction terms between other fields and the gauge bosons,

and therefore also the interactions mediated by the gauge bosons. The covariant derivative becomes

$$\begin{aligned} D_\mu &= \partial_\mu - \mathrm{i} g_1 Q_1 A_\mu^1 - \mathrm{i} g_2 Q_2 A_\mu^2 = \partial_\mu - \mathrm{i}\begin{bmatrix} Q_1 & Q_2 \end{bmatrix} \begin{bmatrix} g_1 & 0 \\ 0 & g_2 \end{bmatrix} \begin{bmatrix} A_\mu^1 \\ A_\mu^2 \end{bmatrix} \\ &= \partial_\mu - \mathrm{i}\begin{bmatrix} Q_1 & Q_2 \end{bmatrix} \begin{bmatrix} g_1 & 0 \\ 0 & g_2 \end{bmatrix} R \begin{bmatrix} B_\mu^1 \\ B_\mu^2 \end{bmatrix} = \partial_\mu - \mathrm{i}\begin{bmatrix} Q_1 & Q_2 \end{bmatrix} G \begin{bmatrix} B_\mu^1 \\ B_\mu^2 \end{bmatrix}. \end{aligned} \tag{2.87}$$

The diagonal matrix containing the two original gauge couplings g_1 and g_2 has then been replaced by the gauge coupling matrix

$$G = \begin{bmatrix} g_1 & 0 \\ 0 & g_2 \end{bmatrix} R = \frac{1}{\sqrt{2}} \begin{bmatrix} \frac{g_1}{\sqrt{1-\chi}} & -\frac{g_1}{\sqrt{1+\chi}} \\ \frac{g_2}{\sqrt{1-\chi}} & \frac{g_2}{\sqrt{1+\chi}} \end{bmatrix} \equiv \begin{bmatrix} g_{11} & g_{12} \\ g_{21} & g_{22} \end{bmatrix}. \tag{2.88}$$

We could stop here, but for the sake of convenience we can note that the kinetic term remains diagonal under orthogonal transformations O of the gauge field basis, since $OO^T = I$. Therefore, if we let

$$\begin{bmatrix} B_\mu^1 \\ B_\mu^2 \end{bmatrix} = \frac{1}{\sqrt{g_{21}^2 + g_{22}^2}} \begin{bmatrix} g_{22} & g_{21} \\ -g_{21} & g_{22} \end{bmatrix} \begin{bmatrix} A_\mu \\ A'_\mu \end{bmatrix} = O \begin{bmatrix} A_\mu \\ A'_\mu \end{bmatrix}, \tag{2.89}$$

where O is the given orthogonal matrix, the kinetic gauge term remains diagonal. The point of this transformation is that if we now insert it into the covariant derivative in Eq. (2.87), we get

$$D_\mu = \partial_\mu - \mathrm{i}\begin{bmatrix} Q_1 & Q_2 \end{bmatrix} GO \begin{bmatrix} A_\mu \\ A'_\mu \end{bmatrix} = \partial_\mu - \mathrm{i}\begin{bmatrix} Q_1 & Q_2 \end{bmatrix} \tilde{G} \begin{bmatrix} A_\mu \\ A'_\mu \end{bmatrix}, \tag{2.90}$$

where the mixing matrix now is

$$\tilde{G} = GO = \begin{bmatrix} g_1 & \frac{\chi g_1}{\sqrt{1-\chi^2}} \\ 0 & \frac{g_2}{\sqrt{1-\chi^2}} \end{bmatrix} \equiv \begin{bmatrix} g & \tilde{g} \\ 0 & g' \end{bmatrix}. \tag{2.91}$$

This basis, where the coupling matrix is triangular, is the one that is usually used for computations. It can be noted that if the mixing is removed by setting $\chi = 0$, this matrix returns to the original diagonal matrix containing only g_1 and g_2.

2.5.2 Matching conditions

When including kinetic mixing, the matching conditions between two groups with multiple Abelian factors take a special form. Let us consider the case where a group consisting of n Abelian factors is broken to a group consisting of n' Abelian factors, where $n' < n$. Following the formalism in Refs. [40, 44], the tree-level matching conditions at the point of symmetry breaking can be written on matrix form as

$$\left(G' G'^T\right)^{-1} = P \left(G G^T\right)^{-1} P^T. \tag{2.92}$$

In this expression, G' is the gauge coupling matrix for the group after symmetry breaking, with n' Abelian factors, while G is the gauge coupling matrix before

symmetry breaking, with n Abelian factors. Also, P is the projection operator of the Abelian charges, describing how the charges of the larger group are combined into the charges of the smaller group. It is worth noting that the expressions in Eq. (2.92) are invariant under orthogonal rotations of the gauge coupling matrix, making it valid whichever basis is chosen.

If a gauge group contains k non-Abelian factors as well, the above matrices simply become a block of a larger gauge coupling matrix, where the non-Abelian couplings are diagonal elements. In that case, we denote the purely Abelian gauge coupling matrix by g, giving

$$\left(GG^T\right)^{-1} = \text{diag}\left((gg^T)^{-1}, \frac{1}{4\pi}\alpha_1^{-1}, \ldots, \frac{1}{4\pi}\alpha_k^{-1}\right), \tag{2.93}$$

where α_i^{-1} denotes the non-Abelian gauge couplings. The projection operator P can then just be filled with zeros and ones, so it leaves these couplings unaffected. The expression in Eq. (2.92) then remains the same.

2.6 Threshold corrections

When considering the matching of coupling constants at symmetry breaking, i.e between an effective theory and a larger one, threshold corrections arise at higher-loop orders [45–47]. When breaking a group $\mathcal{G}_m$ to a subgroup $\mathcal{G}_n$ at a scale $M_{m\to n}$, the matching condition with threshold corrections becomes

$$\alpha_n^{-1}\left(M_{m\to n}\right) = \alpha_m^{-1}\left(M_{m\to n}\right) - \frac{\lambda_n^m}{12\pi}\,. \tag{2.94}$$

If the matching condition contains a linear combination of different couplings, each term gets the corresponding correction, in the sense that each term $\alpha_n^{-1}\left(M_{m\to n}\right)$ in the tree-level matching condition is exchanged for $\alpha_n^{-1}\left(M_{m\to n}\right) + \frac{\lambda_n^m}{12\pi}$. We have, to one-loop order [30],

$$\lambda_n^m = \sum_{i\in\text{vectors}} k_{V_i} C\left(V_i\right) + \sum_{i\in\text{scalars}} \kappa_{S_i} k_{S_i} C\left(S_i\right) \ln\left(\frac{M_{S_i}}{M_{m\to n}}\right). \tag{2.95}$$

Here, V_i and S_i denote representations of vector and scalar fields, respectively, while k_{V_i} and k_{S_i} are the total numbers of dimensions those fields have, as part of other group representations. Also, κ_{S_i} is a factor accounting for that scalar particles can be real or complex, taking the value 1 or 2 for the respective cases. We assume that there are no superheavy fermions, as well as that superheavy vector bosons have masses that are the same as the symmetry breaking scale. This is why there is no

fermion term, and no scale dependence in the vector boson term. For readability, we let

$$\eta_i \equiv \ln\left(\frac{M_{S_i}}{M_{m\to n}}\right), \tag{2.96}$$

which means that

$$\lambda_n^m = \sum_{i\in\text{vectors}} k_{V_i} C(V_i) + \sum_{i\in\text{scalars}} \kappa_{S_i} k_{S_i} C(S_i)\,\eta_i\,. \tag{2.97}$$

For the case when we include the effects of kinetic mixing, and consider the matching conditions discussed in section 2.5.2, the most general expression for the threshold corrections take a more complicated form, as shown in Ref. [48]. However, when we consider the breaking of two Abelian groups to one Abelian group, as will be the case for one of the models analyzed later, the expression in Eq. (2.94) can still be used.

The parameters η_i have physical significance, since they determine how large the masses M_{S_i} of the scalar fields are in relation to the symmetry breaking scale $M_{m\to n}$. Specifically, we get

$$M_{S_i} = M_{m\to n}\mathrm{e}^{\eta_i}\,. \tag{2.98}$$

In order for fields to be relevant for the threshold corrections, they need to have masses close to the symmetry breaking scale. For that reason, we usually want to limit the size of the values of η_i. For example, $\eta_i \in [-3,3]$ roughly corresponds to masses within one order of magnitude from the symmetry breaking scale. How viable a model is can then be determined from how large η_i has to be in order to achieve unification.

2.7 Proton decay

When creating new models, it is essential that they are verified by some kind of experimental data. This poses a problem when creating GUTs, since such theories are valid at much higher energies than those that can be achieved in accelerators in the foreseeable future. Fortunately, even though it might not be possible to observe the GUT couplings directly, there are remnants left behind when the GUT is broken down to the SM at lower energies. One very important possible smoking gun of GUTs is the observation of proton decay. Several currently running experiments are looking for proton decay, but to no avail. This non-observation puts a lower bound on the proton lifetime in different decay channels, for it to be sufficiently probable that no decay has been observed. From the Super-Kamiokande observatory [49, 50], we have the bounds

$$\begin{cases} \tau\left(p\to e^+\pi^0\right) > 1.67\times10^{34}\,\text{yr} \\ \tau\left(p\to \mu^+\pi^0\right) > 7.78\times10^{33}\,\text{yr} \\ \tau\left(p\to \nu K^+\right) > 6.61\times10^{33}\,\text{yr} \end{cases}. \tag{2.99}$$

In the SM, protons are completely stable and cannot decay. However, when looking at GUTs, proton decays are possible—being mediated by the exotic particles appearing in those larger theories. What is needed is some kind particle mediating an interaction between leptons and quarks, which violates baryon number conservation. Such particles are usually called leptoquarks. In SO(10), the proton decay can be mediated by leptoquark gauge bosons coming from the adjoint representation **45**. The interaction then comes from the Dirac term in the Lagrangian, given by

$$\mathcal{L}_{\text{Dirac}} = \mathrm{i}\bar{\psi}\not{D}\psi\,, \tag{2.100}$$

where $\psi \sim \mathbf{16}_{\text{F}}$. The covariant derivative in SO(10) is

$$D_\mu = \partial_\mu - \mathrm{i}g_{10}G^a_\mu T^a\,, \tag{2.101}$$

where g_{10} is the single gauge coupling, T^a are the group generators, and G^a_μ are the gauge boson fields. Since the $\mathbf{16}_{\text{F}}$ contains all SM fermions, this term gives the necessary interactions. The decay can also be mediated by leptoquark scalars, in the Yukawa sector. One example of a tree-level Feynman diagram for proton decay is then shown in Eq. (2.102), where X denotes one of the leptoquark gauge bosons. This diagram illustrates the decay channel $p \to e^+\pi^0$, which is the one with the most constraining experimental bound.

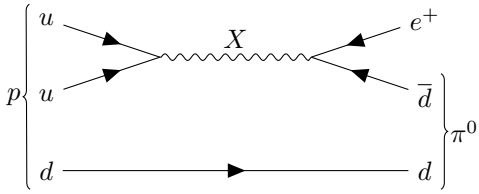

(2.102)

We can then find the approximate decay rate in this channel with the highest lower bound, given by the expression [51, 52]

$$\Gamma\left(p \to e^+\pi^0\right) \simeq \frac{m_p}{64\pi f_\pi^2}\frac{g_{\text{GUT}}^4}{M_{\text{GUT}}^4}A_L^2\alpha_{\text{H}}^2F_q\,. \tag{2.103}$$

Here, $f_\pi \approx 139\,\text{MeV}$ is the pion decay constant, $A_L \approx 2.726$ is a renormalization factor, $\alpha_{\text{H}} \approx 0.012\,\text{GeV}^3$ is the hadronic matrix element, and $F_q \approx 7.6$ accounts for quark mixing. Also, $m_p \approx 938.27\,\text{MeV}$ is the proton mass value from Ref. [31], and $g_{\text{GUT}} \equiv g_{10}(M_{\text{GUT}})$ is the single gauge coupling at M_{GUT}. Since the lifetime of the proton (just based on the decay in this particular channel) is the inverse of the corresponding decay rate, i.e.

$$\tau\left(p \to e^+\pi^0\right) = \frac{1}{\Gamma\left(p \to e^+\pi^0\right)}\,, \tag{2.104}$$

inserting the numerical factors gives the condition

$$\tau\left(p \to e^+\pi^0\right) \simeq \left(7.47 \times 10^{35}\text{yr}\right)\left(\frac{M_{\text{GUT}}}{10^{16}\text{GeV}}\right)^4\left(\frac{\alpha_{\text{GUT}}^{-1}}{33.3}\right)^2\,. \tag{2.105}$$

We can then use this expression together with the experimental bounds given in Eq. (2.99), to put a limit on M_{GUT}. However, this limit also depends on the value of the coupling constant of the unification gauge group SO(10), at the scale of unification. The value of $\alpha_{\mathrm{GUT}}^{-1} = \frac{4\pi}{g_{\mathrm{GUT}}^2}$ may differ for different combinations of the two scales M_{I} and M_{GUT}. Consequently, this constraint does technically not result in a fixed lowest allowed value of M_{GUT}. However, we will see later that the value of α_{GUT} almost only depends on M_{GUT}, giving what effectively is a lower limit for M_{GUT}.

Chapter 3

Description of models

In this thesis, two different SO(10)-based models will be investigated. The two specific breaking chains that define these models are

$$\mathrm{SO}(10) \to \mathrm{SU}(5) \times \mathrm{U}(1)_X \to \mathcal{G}_{\mathrm{SM}}\,, \tag{3.1}$$

as well as

$$\mathrm{SO}(10) \to \mathrm{SU}(3)_{\mathrm{C}} \times \mathrm{SU}(2)_{\mathrm{L}} \times \mathrm{U}(1)_R \times \mathrm{U}(1)_{B-L} \to \mathcal{G}_{\mathrm{SM}}\,. \tag{3.2}$$

The breaking of the GUT group into the intermediate gauge group happens at the so-called unification scale, denoted by $\mu = M_{\mathrm{GUT}}$. That is the point where the different couplings unify into one. The intermediate symmetry is then broken down to the SM at a lower scale $\mu = M_{\mathrm{I}}$, called the intermediate scale. At each symmetry breaking scale, the different couplings from the groups involved are related by matching conditions. These conditions form a system of equations, that we can solve to find the two symmetry breaking scales.

These two are not the only possible ways of breaking SO(10) to $\mathcal{G}_{\mathrm{SM}}$. What makes these two particular breaking chains stand out from the others is that, as we will see later, it is not possible to achieve unification at M_{GUT} without threshold corrections. This makes them especially interesting cases to study, since we can investigate if impossible models can be saved by adding these corrections. We will also examine the effects of kinetic mixing, in the second model. Throughout the rest of this chapter, the properties of these two intermediate gauge groups will be investigated, and the problems that prevent unification within them will be brought to light.

When placing the scalar fields in these models, we will follow the extended survival hypothesis [53], stating that the only scalars at a given scale are those that will later take a VEV. This is a way of building a model in a minimalistic way. It is worth noting that this is not the only way of creating models with these intermediate symmetries, and changing the particle content may change the results.

3.1 Model 1: The flipped SU(5) group

The first of the intermediate gauge groups is given by

$$\mathcal{G}_{51} = \mathrm{SU}(5) \times \mathrm{U}(1)_X \,, \tag{3.3}$$

which is sometimes referred to as the flipped SU(5) group [54–56]. An important note to make is that the SM hypercharge now becomes

$$Y = \frac{1}{5}(X - Y') \,, \tag{3.4}$$

where X is the Abelian charge from $\mathrm{U}(1)_X$, and Y' is the Abelian charge from within SU(5). This charge assignment is what characterizes the flipped SU(5) model, as it forces mixing between the two groups. Without it, the problem would just be reduced to unifying the SM couplings at M_{I}.

3.1.1 Particle content

Similarly to when we just had SU(5), the fermions are embedded in this group as

$$\mathbf{10}_1 \oplus \overline{\mathbf{5}}_{-3} \oplus \mathbf{1}_5 \,, \tag{3.5}$$

where the boldface numbers again denote the representation of the field under SU(5), and the subscript is the Abelian charge from $\mathrm{U}(1)_X$. The fermion representations are then broken down into representations under $\mathcal{G}_{\mathrm{SM}}$, using the hypercharge embedding in Eq. (3.4). We then get

$$\begin{aligned} \mathbf{10}_1 &\to (\overline{\mathbf{3}}, \mathbf{1})_{1/3} \oplus (\mathbf{3}, \mathbf{2})_{1/6} \oplus (\mathbf{1}, \mathbf{1})_0 = d_R^c \oplus Q_L \oplus (\mathbf{1}, \mathbf{1})_0 \,, \\ \overline{\mathbf{5}}_{-3} &\to (\overline{\mathbf{3}}, \mathbf{1})_{-2/3} \oplus (\mathbf{1}, \mathbf{2})_{-1/2} = u_R^c \oplus L_L \,, \\ \mathbf{1}_5 &\to (\mathbf{1}, \mathbf{1})_1 = \ell_R^c \,. \end{aligned} \tag{3.6}$$

We can note a few differences, compared to having only SU(5) as the gauge group. First of all, we see that some of the SM fermion representations have changed places—giving the group its name. The fields u_R^c and d_R^c have swapped their places in the 10- and 5-dimensional representations. Also, we must have a third representation under $\mathcal{G}_{51}$, the $\mathbf{1}_5$, which now decomposes into the right-handed lepton singlet. In its previous place, there is now a SM neutral representation $(\mathbf{1}, \mathbf{1})_0$. This can be seen as the right-handed neutrino that is missing in the SM. Following the earlier reasoning, we now have scalars in the representations

$$\mathbf{5}_{-2} \oplus \mathbf{24}_0 \oplus \overline{\mathbf{50}}_2 \oplus \mathbf{45}_{-2} \,, \tag{3.7}$$

while the vector bosons are in $\mathbf{24}_0$. We see that

$$\mathbf{5}_{-2} \to (\mathbf{3}, \mathbf{1})_{-1/3} \oplus (\mathbf{1}, \mathbf{2})_{1/2} = (\mathbf{3}, \mathbf{1})_{-1/3} \oplus \Phi \,, \tag{3.8}$$

which means that the $\mathbf{5}_{-2}$ is needed to reproduce the SM Higgs. The other scalars are the ones taking VEVs, which are required for symmetry breaking. When this group is considered as an intermediate symmetry below SO(10), we can note that

$$\mathbf{16}_{\mathrm{F}} \to \mathbf{10}_1 \oplus \overline{\mathbf{5}}_{-3} \oplus \mathbf{1}_5\,, \tag{3.9}$$

which is what we would expect.

3.1.2 Charge normalization

When considering the group $\mathcal{G}_{51}$ as an intermediate symmetry between the SM and SO(10), there are two Abelian charges that require normalizing. First, the charge X, coming from the group factor $\mathrm{U}(1)_X$. From Eq. (3.9), we see how the fermion representation breaks down, which means that

$$\mathrm{Tr}\big[X^2\big] = 10(1)^2 + 5(-3)^2 + 1(5)^2 = 80\,. \tag{3.10}$$

From Eq. (2.62) we get the normalization condition

$$\mathrm{Tr}\big[T^a T^b\big] = C(\mathbf{16})\delta^{ab} = 2\delta^{ab}\,, \tag{3.11}$$

for generators in the representation $\mathbf{16}_{\mathrm{F}}$, and normalizing one of the SO(10) generators as $T^i = k_X X$, we then get

$$2 = k_X^2\,\mathrm{Tr}\big[X^2\big] = 80k_X^2 \quad \Longrightarrow \quad k_X = \frac{1}{\sqrt{40}}\,. \tag{3.12}$$

Furthermore, we need to normalize the hypercharge

$$Y = \frac{1}{5}(X - Y')\,, \tag{3.13}$$

where Y' is the Abelian charge from within SU(5). Taking into account the corresponding values of Y' for the representations in Eq. (3.6), we get for the $\mathbf{16}_{\mathrm{F}}$ in SO(10),

$$\begin{aligned}\mathrm{Tr}\big[Y^2\big] = \frac{1}{25}\Bigg[6\left(1-\frac{1}{6}\right)^2 + 3\left(1-\left(-\frac{2}{3}\right)\right)^2 + 1(1-1)^2 \\ + 3\left(-3-\frac{1}{3}\right)^2 + 2\left(-3-\left(-\frac{1}{2}\right)\right)^2 + 1(5-0)^2\Bigg] = \frac{10}{3}\,,\end{aligned} \tag{3.14}$$

which is reasonable considering that the representations were just moved around, as compared to the SU(5) group. Normalizing another generator of SO(10) as $T^j = k_Y Y$, we then again get

$$2 = k_Y^2\,\mathrm{Tr}\big[Y^2\big] = \frac{10}{3}k_Y^2 \quad \Longrightarrow \quad k_Y = \sqrt{\frac{3}{5}}\,, \tag{3.15}$$

giving the same hypercharge normalization as earlier.

3.1.3 Running of couplings

Since this group only contains two simple factors, there are only two gauge couplings that need to be considered. As we will see later on, this simplifies the model quite a bit, as both the number of equations and the number of coefficients are reduced. Looking at the β-function coefficients for the running of these two coupling constants, we get to one-loop order

$$b = \begin{bmatrix} b_{1X} & b_5 \end{bmatrix} = \begin{bmatrix} \frac{22}{3} & \frac{8}{3} \end{bmatrix}, \tag{3.16}$$

where the indices $1X$ and 5 now instead refer to the couplings corresponding to $\mathrm{U}(1)_X$ and SU(5), respectively. Inserting this in Eq. (2.46), we can then write out the analytical one-loop solutions as

$$\begin{aligned} \alpha_{1X}^{-1} &= -\frac{11}{3\pi}\log\left(\frac{Q}{M_\mathrm{I}}\right) + \alpha_{1X}^{-1}(M_\mathrm{I}), \\ \alpha_5^{-1} &= -\frac{4}{3\pi}\log\left(\frac{Q}{M_\mathrm{I}}\right) + \alpha_5^{-1}(M_\mathrm{I}). \end{aligned} \tag{3.17}$$

Also, the coefficients for the two-loop β-functions now become

$$B = \begin{bmatrix} B_{1X,1X} & B_{1X,5} \\ B_{5,1X} & B_{5,5} \end{bmatrix} = \begin{bmatrix} \frac{79}{10} & \frac{1548}{5} \\ \frac{129}{10} & \frac{14594}{15} \end{bmatrix}. \tag{3.18}$$

Let us then look at the matching conditions at the two different points where symmetry breaking occurs. At the intermediate scale M_I, we have

$$\begin{cases} \alpha_{1X}^{-1}(M_\mathrm{I}) = \frac{1}{24}\left(25\alpha_{1Y}^{-1}(M_\mathrm{I}) - \alpha_{2\mathrm{L}}^{-1}(M_\mathrm{I})\right) \\ \alpha_5^{-1}(M_\mathrm{I}) = \alpha_{2\mathrm{L}}^{-1}(M_\mathrm{I}) \\ \alpha_5^{-1}(M_\mathrm{I}) = \alpha_{3\mathrm{C}}^{-1}(M_\mathrm{I}) \end{cases}. \tag{3.19}$$

We can note something interesting here, which is unique for this model and a result of that both of the non-Abelian factors in $\mathcal{G}_\mathrm{SM}$ originate from the single SU(5) factor. That is that $\alpha_5^{-1}(M_\mathrm{I})$ can be eliminated from the two last equations of this system, resulting in the system

$$\begin{cases} \alpha_{1X}^{-1}(M_\mathrm{I}) = \frac{1}{24}\left(25\alpha_{1Y}^{-1}(M_\mathrm{I}) - \alpha_{2\mathrm{L}}^{-1}(M_\mathrm{I})\right) \\ \alpha_{3\mathrm{C}}^{-1}(M_\mathrm{I}) - \alpha_{2\mathrm{L}}^{-1}(M_\mathrm{I}) = 0 \end{cases}. \tag{3.20}$$

Therefore, the intermediate scale M_I can be found just from the second equation alone, and is consequently uniquely determined by the running of the SM couplings, as it is the scale of the intersection between the two non-Abelian couplings in the

SM. An analytical expression can be found for the intermediate scale, in the one-loop case. Inserting the one-loop SM solutions from Eq. (2.54) into the second equation in Eq. (3.20), we get

$$\frac{19}{12\pi}\ln\left(\frac{M_{\rm I}}{M_{\rm Z}}\right)+\alpha_{\rm 2L}^{-1}(M_{\rm Z})=\frac{7}{2\pi}\ln\left(\frac{M_{\rm I}}{M_{\rm Z}}\right)+\alpha_{\rm 3C}^{-1}(M_{\rm Z})\,, \tag{3.21}$$

which gives

$$M_{\rm I}=M_{\rm Z}\exp\left\{\frac{12\pi}{23}\left[\alpha_{\rm 2L}^{-1}(M_{\rm Z})-\alpha_{\rm 3C}^{-1}(M_{\rm Z})\right]\right\}. \tag{3.22}$$

The same equation can also be solved for $M_{\rm I}$ in the two-loop case, but must instead be done so numerically. Inserting the SM initial values in Eq. (3.22), and doing the numerical computations, we find the two different values of $M_{\rm I}$ shown in table 3.1.

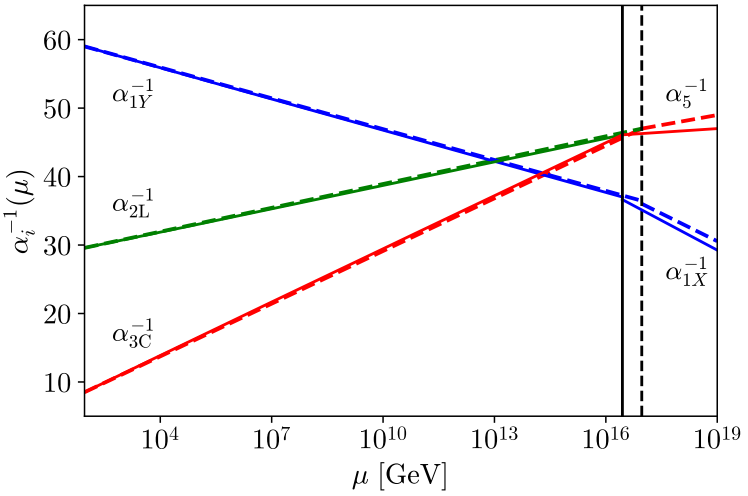

Figure 3.1: The running of the gauge couplings when $\mathcal{G}_{51}$ is broken to the SM gauge group, to one-loop order (dashed) and two-loop order (solid). The plot also shows, as vertical lines, the fixed intermediate scales $M_{\rm I}$ from table 3.1 where the symmetry breaking occurs.

	One-loop	Two-loop
$M_{\rm I}$[GeV]	9.28×10^{16}	2.74×10^{16}

Table 3.1: The intermediate scale $M_{\rm I}$ where $\mathcal{G}_{51}$ is broken into $\mathcal{G}_{\rm SM}$.

Figure 3.1 shows the running of the coupling constants corresponding to these solutions. What we can see is that at scales higher than $M_{\rm I}$, α_{1X}^{-1} and α_5^{-1} just

go further apart, and will continue doing so. Since we want unification at a scale larger than M_{I}, this is a bad sign. We cannot achieve unification of the couplings by simply placing the two scales M_{I} and M_{GUT} appropriately. Thus, there is not really any point in looking at the matching conditions at the unification scale, since it is clear there is no solution for $M_{\mathrm{GUT}} > M_{\mathrm{I}}$. It would seem like this model needs to be discarded, but as we will see later, it is possible to save it by considering threshold corrections at the different symmetry breaking scales.

3.2 Model 2: The SU(3) × SU(2) × U(1) × U(1) group

The other intermediate gauge group that will be treated is

$$\mathcal{G}_{3211} = \mathrm{SU}(3)_{\mathrm{C}} \times \mathrm{SU}(2)_{\mathrm{L}} \times \mathrm{U}(1)_R \times \mathrm{U}(1)_{B-L}\,, \tag{3.23}$$

which is discussed in e.g. Refs. [57, 58]. We can note that this group is very similar to the gauge group $\mathcal{G}_{\mathrm{SM}}$ of the SM, as the only difference is that there are now two different Abelian charges. This similarity can also be seen in the different particle representations, and will have interesting effects on the later analysis. When breaking $\mathcal{G}_{3211}$ down to $\mathcal{G}_{\mathrm{SM}}$, the representations under the non-Abelian group factors are left unchanged, while the two Abelian charges mix according to

$$Y = \frac{B-L}{2} - R\,, \tag{3.24}$$

to form the SM hypercharge Y.

3.2.1 Particle content

The fermions are embedded as

$$(\mathbf{3},\mathbf{2})_{0,\frac{1}{3}} \oplus (\mathbf{1},\mathbf{2})_{0,-1} \oplus (\overline{\mathbf{3}},\mathbf{1})_{-\frac{1}{2},-\frac{1}{3}} \oplus (\overline{\mathbf{3}},\mathbf{1})_{\frac{1}{2},-\frac{1}{3}} \oplus (\mathbf{1},\mathbf{1})_{\frac{1}{2},1} \oplus (\mathbf{1},\mathbf{1})_{-\frac{1}{2},1}\,, \tag{3.25}$$

where the two boldface numbers again denote the representations under $\mathrm{SU}(3)_{\mathrm{C}}$ and $\mathrm{SU}(2)_{\mathrm{L}}$, respectively, while the first subscript is the Abelian charge R, and the second subscript is the Abelian charge $B-L$. Following the hypercharge embedding in Eq. (3.24), we find that these representations decompose as

$$\begin{aligned}
(\mathbf{3},\mathbf{2})_{0,\frac{1}{3}} &\to (\mathbf{3},\mathbf{2})_{1/6} = Q_L\,,\\
(\mathbf{1},\mathbf{2})_{0,-1} &\to (\mathbf{1},\mathbf{2})_{-1/2} = L_L\,,\\
(\overline{\mathbf{3}},\mathbf{1})_{-\frac{1}{2},-\frac{1}{3}} &\to (\overline{\mathbf{3}},\mathbf{1})_{\frac{1}{3}} = d_R^c\,,\\
(\overline{\mathbf{3}},\mathbf{1})_{\frac{1}{2},-\frac{1}{3}} &\to (\overline{\mathbf{3}},\mathbf{1})_{-2/3} = u_R^c\,,\\
(\mathbf{1},\mathbf{1})_{\frac{1}{2},1} &\to (\mathbf{1},\mathbf{1})_{1} = \ell_R^c\,,\\
(\mathbf{1},\mathbf{1})_{-\frac{1}{2},1} &\to (\mathbf{1},\mathbf{1})_{0}\,.
\end{aligned} \tag{3.26}$$

Furthermore, we have scalar representations at the intermediate scale

$$(\mathbf{1},\mathbf{2})_{-\frac{1}{2},0} \oplus (\mathbf{1},\mathbf{1})_{1,2} \oplus (\mathbf{1},\mathbf{2})_{-\frac{1}{2},0}\,, \tag{3.27}$$

where we see that

$$(\mathbf{1},\mathbf{2})_{-\frac{1}{2},0} \to (\mathbf{1},\mathbf{2})_{\frac{1}{2}} = \Phi \tag{3.28}$$

reproduces the scalar SM Higgs, while the other representations are needed for the symmetry breaking itself. When this group is considered as an intermediate symmetry below SO(10), we find that

$$\mathbf{16}_F \to (\mathbf{3},\mathbf{2})_{0,\frac{1}{3}} \oplus (\mathbf{1},\mathbf{2})_{0,-1} \oplus (\overline{\mathbf{3}},\mathbf{1})_{-\frac{1}{2},-\frac{1}{3}} \oplus (\overline{\mathbf{3}},\mathbf{1})_{\frac{1}{2},-\frac{1}{3}} \oplus (\mathbf{1},\mathbf{1})_{\frac{1}{2},1} \oplus (\mathbf{1},\mathbf{1})_{-\frac{1}{2},1}\,, \tag{3.29}$$

which again agrees with what we would expect.

3.2.2 Charge normalization

When treating models based on the gauge group $\mathcal{G}_{3211}$, there are again two Abelian charges, R and $B-L$, that need to be normalized correctly. This can again be done by observing how the representation $\mathbf{16}_\mathrm{F}$, containing all of the fermions, decomposes to representations under $\mathcal{G}_{3211}$ in Eq. (3.29). For both charges, we can again use the condition

$$\mathrm{Tr}[(T^i)^2] = C(\mathbf{16}) = 2\,. \tag{3.30}$$

Let us first look at the charge R, for which we get

$$\mathrm{Tr}[R^2] = 6(0)^2 + 2(0)^2 + 3\left(-\frac{1}{2}\right)^2 + 3\left(\frac{1}{2}\right)^2 + \left(\frac{1}{2}\right)^2 + \left(-\frac{1}{2}\right)^2 = 2\,. \tag{3.31}$$

As a result, it does not require any normalizing. For the second Abelian charge $B-L$, we instead get

$$\mathrm{Tr}[(B-L)^2] = 6\left(\frac{1}{3}\right)^2 + 2(-1)^2 + 3\left(-\frac{1}{3}\right)^2 + 3\left(-\frac{1}{3}\right)^2 + (1)^2 + (1)^2 = \frac{16}{3}\,. \tag{3.32}$$

As this is not properly normalized, we can insert a normalization factor so that

$$T^i = k_{B-L}(B-L)\,, \tag{3.33}$$

which then gives

$$2 = k_{B-L}^2\,\mathrm{Tr}\big[(B-L)^2\big] = \frac{16}{3}k_{B-L}^2 \quad \Longrightarrow \quad k_{B-L} = \sqrt{\frac{3}{8}}\,. \tag{3.34}$$

3.2.3 Running of couplings

This gauge group contains four simple factors, which means that there are now four gauge couplings. This case therefore becomes a bit more complicated to deal with, compared to the previous one. Using the representations of the particle content discussed earlier, we find that

$$b = \begin{bmatrix} b_{1B-L} & b_{1R} & b_{2\mathrm{L}} & b_{3\mathrm{C}} \end{bmatrix} = \begin{bmatrix} \frac{9}{2} & \frac{14}{3} & -3 & -7 \end{bmatrix}, \tag{3.35}$$

where the subscripts $1B-L$ and $1R$ refer to the two different Abelian couplings, and the indices 2L and 3C again refer to the couplings corresponding to $\mathrm{SU}(2)_{\mathrm{L}}$ and $\mathrm{SU}(3)_{\mathrm{C}}$, respectively. Inserting into Eq. (2.46), we get the analytical one-loop solutions

$$\begin{aligned} \alpha_{1B-L}^{-1} &= -\frac{9}{4\pi}\log\left(\frac{Q}{M_{\mathrm{I}}}\right) + \alpha_{1B-L}^{-1}(M_{\mathrm{I}}), \\ \alpha_{1R}^{-1} &= -\frac{7}{3\pi}\log\left(\frac{Q}{M_{\mathrm{I}}}\right) + \alpha_{1R}^{-1}(M_{\mathrm{I}}), \\ \alpha_{2\mathrm{L}}^{-1} &= \frac{3}{2\pi}\log\left(\frac{Q}{M_{\mathrm{I}}}\right) + \alpha_{2\mathrm{L}}^{-1}(M_{\mathrm{I}}), \\ \alpha_{3\mathrm{C}}^{-1} &= \frac{7}{2\pi}\log\left(\frac{Q}{M_{\mathrm{I}}}\right) + \alpha_{3\mathrm{C}}^{-1}(M_{\mathrm{I}}). \end{aligned} \tag{3.36}$$

Now, the 16 different coefficients for the two-loop β-functions are given by

$$B = \begin{bmatrix} B_{1B-L,1B-L} & B_{1B-L,1R} & B_{1B-L,2\mathrm{L}} & B_{1B-L,3\mathrm{C}} \\ B_{1R,1B-L} & B_{1R,1R} & B_{1R,2\mathrm{L}} & B_{1R,3\mathrm{C}} \\ B_{2\mathrm{L},1B-L} & B_{2\mathrm{L},1R} & B_{2\mathrm{L},2\mathrm{L}} & B_{2\mathrm{L},3\mathrm{C}} \\ B_{3\mathrm{C},1B-L} & B_{3\mathrm{C},1R} & B_{3\mathrm{C},2\mathrm{L}} & B_{3\mathrm{C},3\mathrm{C}} \end{bmatrix} = \begin{bmatrix} \frac{25}{2} & \frac{15}{2} & \frac{9}{2} & 4 \\ \frac{15}{2} & 8 & 3 & 12 \\ \frac{3}{2} & 1 & 8 & 12 \\ \frac{1}{2} & \frac{3}{2} & \frac{9}{2} & -26 \end{bmatrix}. \tag{3.37}$$

Let us then look at the matching conditions at the point of symmetry breaking. At the intermediate scale M_{I}, we get

$$\begin{cases} \alpha_{1Y}^{-1}(M_{\mathrm{I}}) = \frac{2}{5}\alpha_{1B-L}^{-1}(M_{\mathrm{I}}) + \frac{3}{5}\alpha_{1R}^{-1}(M_{\mathrm{I}}) \\ \alpha_{2\mathrm{L}}^{-1}(M_{\mathrm{I}}) = \alpha_{2\mathrm{L}}^{-1}(M_{\mathrm{I}}) \\ \alpha_{3\mathrm{C}}^{-1}(M_{\mathrm{I}}) = \alpha_{3\mathrm{C}}^{-1}(M_{\mathrm{I}}) \end{cases}. \tag{3.38}$$

However, we encounter a problem here, which stems from that we are matching three couplings (for scales below M_{I}) to four couplings (for scales above M_{I}). Written in the way it is in Eq. (3.38), the system of equations for matching gives a unique solution, as long as we are finding the SM couplings from the given $\mathcal{G}_{3211}$ couplings. However, just like in the previous case, our initial values from experimental data are given at M_{Z}, which means that the system must be solved from lower scales and up. Unfortunately, the system of equations is not uniquely invertible, since

many different combinations of $\alpha_{1B-L}^{-1}(M_\mathrm{I})$ and $\alpha_{1R}^{-1}(M_\mathrm{I})$ can give the same value of $\alpha_{1Y}^{-1}(M_\mathrm{I})$. One way of fixing this is to insert an extra equation, such as

$$\alpha_{1B-L}^{-1}(M_\mathrm{I}) = x\alpha_{1R}^{-1}(M_\mathrm{I})\,, \tag{3.39}$$

where x now is another variable to be solved for, along with M_I. With this extra equation, the system can be inverted and written as

$$\begin{cases} \alpha_{1B-L}^{-1}\left(M_1\right) = x\left(\frac{2}{5}x + \frac{3}{5}\right)^{-1}\alpha_{1Y}^{-1}\left(M_\mathrm{I}\right) \\ \alpha_{1R}^{-1}\left(M_\mathrm{I}\right) = \left(\frac{2}{5}x + \frac{3}{5}\right)^{-1}\alpha_{1Y}^{-1}\left(M_\mathrm{I}\right) \\ \alpha_{2\mathrm{L}}^{-1}(M_\mathrm{I}) = \alpha_{2\mathrm{L}}^{-1}(M_\mathrm{I}) \\ \alpha_{3\mathrm{C}}^{-1}(M_\mathrm{I}) = \alpha_{3\mathrm{C}}^{-1}(M_\mathrm{I}) \end{cases}. \tag{3.40}$$

It is important to keep in mind that x does not correspond to some physical quantity, but is rather just a remnant of forcing the system to be invertible in the way we need it to be. Therefore, it results in a system that has an infinite number of solutions, each one depending on the value of x. During the later analysis, we will be able to remove the dependence on this parameter.

Unlike in the previous case with $\mathcal{G}_{51}$, these matching conditions are not enough to solve for the intermediate scale M_I. We can immediately identify a problem standing in the way of unification for this model—namely that the slopes of α_{1B-L}^{-1} and α_{1R}^{-1}, corresponding to the two Abelian couplings, are very similar. As a result, it is difficult to find an intersection between the two, unless they start at very similar initial values at M_I. This would correspond to a value of x near 1. However, then those two Abelian couplings pass nowhere near the intersection between $\alpha_{2\mathrm{L}}^{-1}$ and $\alpha_{3\mathrm{C}}^{-1}$, as seen in figure 3.2c. It is still possible to get one of the Abelian couplings to unify with the two non-Abelian ones, by modifying the value of x. This is also shown in figure 3.2, for $x = 1.4$ and $x = 0.6$. Unfortunately, the price that must be paid for moving one of the Abelian couplings so that it reaches the common intersection of $\alpha_{2\mathrm{L}}^{-1}$ and $\alpha_{3\mathrm{C}}^{-1}$ is that the other one gets pushed too far down, in order to still satisfy the relation

$$\alpha_{1Y}^{-1}(M_\mathrm{I}) = \frac{2}{5}\alpha_{1B-L}^{-1}(M_\mathrm{I}) + \frac{3}{5}\alpha_{1R}^{-1}(M_\mathrm{I})\,. \tag{3.41}$$

In all of these plots, the intermediate scale M_I is chosen (rather arbitrarily) to be $M_\mathrm{I} = 10^{10}\,\mathrm{GeV}$. Setting it differently changes the plots, although the general behavior remains the same. Thus, we find that it is not possible to achieve unification in the model, at tree-level matching.

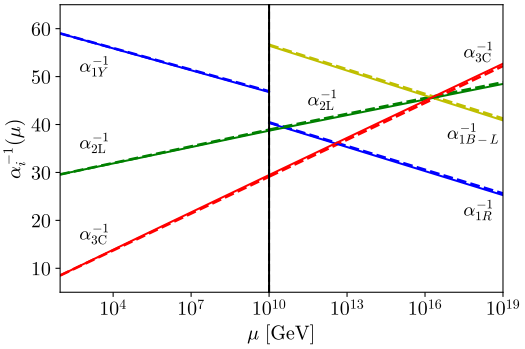

(a) $x = 1.4$.

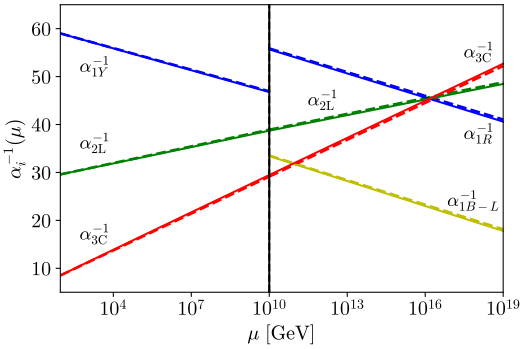

(b) $x = 0.6$.

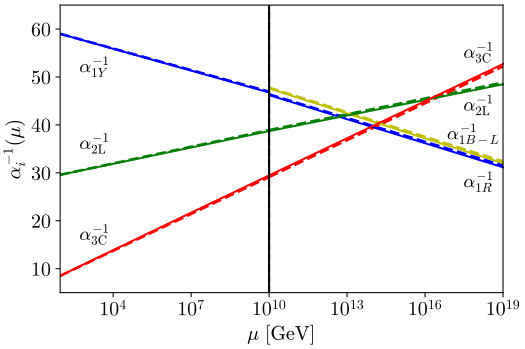

(c) $x = 1.03$.

Figure 3.2: The running of the gauge couplings when $\mathcal{G}_{3211}$ is broken to the SM gauge group, to one-loop order (dashed) and two-loop order (solid). The plots also show, as vertical lines, the intermediate scale $M_{\rm I}$ where $\mathcal{G}_{3211}$ is broken to the SM. Here, the intermediate scale is chosen to be $M_{\rm I} = 10^{10}$ GeV, while x takes three different values.

3.2.4 Adding kinetic mixing

When we have $\mathcal{G}_{3211}$ as the intermediate symmetry group, kinetic mixing can occur between $M_{\rm I}$ and $M_{\rm GUT}$, since we have two different Abelian factors. Following the earlier discussion in section 2.5, we will be working in the basis where the gauge coupling matrix is triangular, where we have $g = g_{1R}$, $g' = g_{1B-L}$, as well as the off-diagonal coupling $\tilde{g}$. The β-functions for these couplings become more complicated than before, and the extra contributions are given below[1]. We will let the superscripts (1) and (2) denote contributions at one- and two-loop order. Note that, just like earlier, the full two-loop function contains both contributions.

[1]The coefficients in these β-functions are computed using the PyR@TE Python package [59–61].

The running of the coupling g_{1R} is only affected at two-loop order, where the additional terms coming from the mixing are

$$\beta_k^{(2)}(g_{1R}) = 8g_{1R}^3\tilde{g}^2 + 4\sqrt{6}g_{1R}^3 g_{1B-L}\tilde{g}\,. \tag{3.42}$$

The β-function for g_{1B-L} is instead affected at both one- and two-loop order, since

$$\begin{aligned}
\beta_k^{(1)}(g_{1B-L}) &= \frac{14}{3}g_{1B-L}\tilde{g}^2 + \frac{\sqrt{6}}{3}g_{1B-L}^2\tilde{g}\,,\\
\beta_k^{(2)}(g_{1B-L}) &= 8g_{1R}^2 g_{1B-L}\tilde{g}^2 + 45g_{1B-L}^3\tilde{g}^2 + 8\sqrt{6}g_{1B-L}^2\tilde{g}^3\\
&\quad + 8g_{1B-L}\tilde{g}^4 + 3g_{2\mathrm{L}}^2 g_{1B-L}\tilde{g}^2 + 12g_{3\mathrm{C}}^2 g_{1B-L}\tilde{g}^2\\
&\quad + 4\sqrt{6}g_{1R}^2 g_{1B-L}^2\tilde{g} + 12\sqrt{6}g_{1B-L}^4\tilde{g}\,.
\end{aligned} \tag{3.43}$$

The two couplings $g_{2\mathrm{L}}$ and $g_{3\mathrm{C}}$ corresponding to the non-Abelian groups also only get extra contributions at two-loop level. We find that

$$\begin{aligned}
\beta_k^{(2)}(g_{2\mathrm{L}}) &= g_{2\mathrm{L}}^3\tilde{g}^2\,,\\
\beta_k^{(2)}(g_{3\mathrm{C}}) &= \frac{3}{2}g_{3\mathrm{C}}^3\tilde{g}^2\,.
\end{aligned} \tag{3.44}$$

Finally, the off-diagonal coupling $\tilde{g}$ has β-function contributions given by

$$\begin{aligned}
\beta_k^{(1)}(\tilde{g}) &= \frac{\sqrt{6}}{3}g_{1R}^2 g_{1B-L} + \frac{\sqrt{6}}{3}g_{1B-L}\tilde{g}^2 + \frac{28}{3}g_{1R}^2\tilde{g} + \frac{9}{2}g_{1B-L}^2\tilde{g} + \frac{14}{3}\tilde{g}^3\,,\\
\beta_k^{(2)}(\tilde{g}) &= 6\sqrt{6}g_{1R}^2 g_{1B-L}^3 + 24g_{1R}^2\tilde{g}^3 + 4\sqrt{6}g_{1R}^4 g_{1B-L} + 16\sqrt{6}g_{1R}^2 g_{1B-L}\tilde{g}^2\\
&\quad + 12\sqrt{6}g_{1B-L}^3\tilde{g}^2 + 45g_{1B-L}^2\tilde{g}^3 + 8\sqrt{6}g_{1B-L}\tilde{g}^4 + 16g_{1R}^4\tilde{g}\\
&\quad + \frac{105}{2}g_{1R}^2 g_{1B-L}^2\tilde{g} + \frac{25}{2}g_{1B-L}^4\tilde{g} + 8\tilde{g}^5 + 6g_{2\mathrm{L}}^2 g_{1R}^2\tilde{g} + \frac{9}{2}g_{2\mathrm{L}}^2 g_{1B-L}^2\tilde{g}\\
&\quad + 24g_{3\mathrm{C}}^2 g_{1R}^2\tilde{g} + 4g_{3\mathrm{C}}^2 g_{1B-L}^2\tilde{g} + 3g_{2\mathrm{L}}^2\tilde{g}^3 + 12g_{3\mathrm{C}}^2\tilde{g}^3\,.
\end{aligned} \tag{3.45}$$

The full two-loop β-function for this coupling then becomes $\beta(\tilde{g}) = \beta_k^{(1)}(\tilde{g}) + \beta_k^{(2)}(\tilde{g})$, since it did not exist before adding kinetic mixing.

We must also look at how the matching conditions between the Abelian couplings change as a result of kinetic mixing. This happens when two Abelian factors are broken into one, so the effects need only be considered at M_{I}. To find the matching condition, we have the SM couplings

$$\left(G'G'^T\right)^{-1} = \frac{1}{4\pi}\begin{bmatrix}\alpha_{1Y}^{-1} & 0 & 0\\ 0 & \alpha_{2\mathrm{L}}^{-1} & 0\\ 0 & 0 & \alpha_{3\mathrm{C}}^{-1}\end{bmatrix}. \tag{3.46}$$

The expression on the right-hand side of Eq. (2.92), corresponding to the $\mathcal{G}_{3211}$ couplings, requires a bit more work. The Abelian part of the gauge coupling matrix

is given by

$$\begin{aligned}\left(gg^T\right)^{-1} &= \left(\begin{bmatrix} g_{1R} & \tilde{g} \\ 0 & g_{1B-L} \end{bmatrix}\begin{bmatrix} g_{1R} & \tilde{g} \\ 0 & g_{1B-L} \end{bmatrix}\right)^{-1} = \begin{bmatrix} g_{1R}^2 & \tilde{g}(g_{1R}+g_{1B-L}) \\ 0 & g_{1B-L}^2 \end{bmatrix}^{-1} \\ &= \begin{bmatrix} g_{1R}^{-2} & -\tilde{g}(g_{1R}+g_{1B-L})g_{1R}^{-2}g_{1B-L}^{-2} \\ 0 & g_{1B-L}^{-2} \end{bmatrix} \\ &= \begin{bmatrix} \frac{1}{4\pi}\alpha_{1R}^{-1} & -\frac{1}{(4\pi)^2}\tilde{g}(g_{1R}+g_{1B-L})\alpha_{1R}^{-1}\alpha_{1B-L}^{-1} \\ 0 & \frac{1}{4\pi}\alpha_{1B-L}^{-1} \end{bmatrix},\end{aligned} \tag{3.47}$$

which then gives

$$\left(GG^T\right)^{-1} = \begin{bmatrix} \left(gg^T\right)^{-1} & 0 & 0 \\ 0 & \frac{1}{4\pi}\alpha_{2\mathrm{L}}^{-1} & 0 \\ 0 & 0 & \frac{1}{4\pi}\alpha_{3\mathrm{C}}^{-1} \end{bmatrix}, \tag{3.48}$$

since the non-Abelian couplings just appear as diagonal elements. Finally, we need to insert the projection operator P. Taking into account the GUT normalizations $\sqrt{\frac{3}{5}}$ of the hypercharge and $\sqrt{\frac{3}{8}}$ of the $B-L$ charge, we have

$$P = \begin{bmatrix} \sqrt{\frac{3}{5}} & \sqrt{\frac{2}{5}} & 0 & 0 \\ 0 & 0 & 1 & 0 \\ 0 & 0 & 0 & 1 \end{bmatrix}. \tag{3.49}$$

Inserting into Eq. (2.92), we then get

$$\begin{aligned}&\frac{1}{4\pi}\begin{bmatrix} \alpha_{1Y}^{-1} & 0 & 0 \\ 0 & \alpha_{2\mathrm{L}}^{-1} & 0 \\ 0 & 0 & \alpha_{3\mathrm{C}}^{-1} \end{bmatrix} \\ &\quad = \begin{bmatrix} \sqrt{\frac{3}{5}} & \sqrt{\frac{2}{5}} & 0 & 0 \\ 0 & 0 & 1 & 0 \\ 0 & 0 & 0 & 1 \end{bmatrix}\begin{bmatrix} \left(gg^T\right)^{-1} & 0 & 0 \\ 0 & \frac{1}{4\pi}\alpha_{2\mathrm{L}}^{-1} & 0 \\ 0 & 0 & \frac{1}{4\pi}\alpha_{3\mathrm{C}}^{-1} \end{bmatrix}\begin{bmatrix} \sqrt{\frac{3}{5}} & 0 & 0 \\ \sqrt{\frac{2}{5}} & 0 & 0 \\ 0 & 1 & 0 \\ 0 & 0 & 1 \end{bmatrix}.\end{aligned} \tag{3.50}$$

Writing out the three different equations given by this matrix relation, we then find that the matching conditions for the non-Abelian couplings are unchanged, i.e.

$$\begin{cases} \alpha_{2\mathrm{L}}^{-1}(M_{\mathrm{I}}) = \alpha_{2\mathrm{L}}^{-1}(M_{\mathrm{I}}) \\ \alpha_{3\mathrm{C}}^{-1}(M_{\mathrm{I}}) = \alpha_{3\mathrm{C}}^{-1}(M_{\mathrm{I}}) \end{cases}. \tag{3.51}$$

However, for the Abelian couplings, we now get

$$\begin{aligned}\alpha_{1Y}^{-1}(M_{\rm I}) &= \frac{3}{5}\alpha_{1R}^{-1} + \frac{2}{5}\alpha_{1B-L}^{-1} - \frac{1}{4\pi}\frac{\sqrt{6}}{5}\tilde{g}(g_{1R}+g_{1B-L})\alpha_{1R}^{-1}\alpha_{1B-L}^{-1} \\ &= \frac{3}{5}\alpha_{1R}^{-1} + \frac{2}{5}\alpha_{1B-L}^{-1} - \frac{\sqrt{6}}{5}\sqrt{\tilde{\alpha}}(\sqrt{\alpha_{1R}}+\sqrt{\alpha_{1B-L}})\alpha_{1R}^{-1}\alpha_{1B-L}^{-1}\,.\end{aligned} \tag{3.52}$$

We can assure ourselves by noting that removing the kinetic mixing by setting $\tilde{\alpha}=0$ in this expression returns

$$\alpha_{1Y}^{-1}(M_{\rm I}) = \frac{2}{5}\alpha_{1B-L}^{-1}(M_{\rm I}) + \frac{3}{5}\alpha_{1R}(M_{\rm I})\,, \tag{3.53}$$

which is the same matching condition as we had earlier, without mixing. Just like then, we need to insert extra equations in order to able to solve this system from lower energies and up. Aside from the condition

$$\alpha_{1B-L}^{-1}\left(M_{\rm I}\right) = x\alpha_{1R}^{-1}\left(M_{\rm I}\right)\,, \tag{3.54}$$

we also need a second condition, for example

$$\alpha_{1R}^{-1}\left(M_{\rm I}\right) = y^2\tilde{\alpha}^{-1}\left(M_{\rm I}\right)\,. \tag{3.55}$$

Again, x and y do not represent any particular physical quantities, and will be removed later during an optimization process. Inserting these two new relations into Eq. (3.52) then gives

$$\begin{aligned}\alpha_{1B-L}^{-1}\left(M_{\rm I}\right) &= x\left(\frac{2}{5}x+\frac{3}{5}-\frac{\sqrt{6}}{5}y\big(x+\sqrt{x}\big)\right)^{-1}\alpha_{1Y}^{-1}\left(M_{\rm I}\right)\,, \\ \alpha_{1R}^{-1}\left(M_{\rm I}\right) &= \left(\frac{2}{5}x+\frac{3}{5}-\frac{\sqrt{6}}{5}y\big(x+\sqrt{x}\big)\right)^{-1}\alpha_{1Y}^{-1}\left(M_{\rm I}\right)\,, \\ \tilde{\alpha}^{-1}\left(M_{\rm I}\right) &= \frac{1}{y^2}\left(\frac{2}{5}x+\frac{3}{5}-\frac{\sqrt{6}}{5}y\big(x+\sqrt{x}\big)\right)^{-1}\alpha_{1Y}^{-1}\left(M_{\rm I}\right)\,.\end{aligned} \tag{3.56}$$

Together with the conditions in Eq. (3.51), Eq. (3.56) provides the matching conditions at $M_{\rm I}$, between $\mathcal{G}_{3211}$ and $\mathcal{G}_{\rm SM}$. The general behavior of the different couplings, and their dependence on the parameter x, is then the same as in the previous section. There is however one striking difference; that the initial conditions of α_{1R}^{-1} and α_{1B-L}^{-1} can be changed by changing the value of the newly inserted parameter y. As shown by the example in figure 3.3, modifying these parameters allows for the couplings to intersect without having any corrections at all. In the plot, couplings with and without kinetic mixing are shown, illustrating the effects of the changed β-functions and the addition of the extra parameter y. Note that

the plot only shows the running to one-loop order to avoid cluttering, but the same manipulation is also possible at two-loop order.

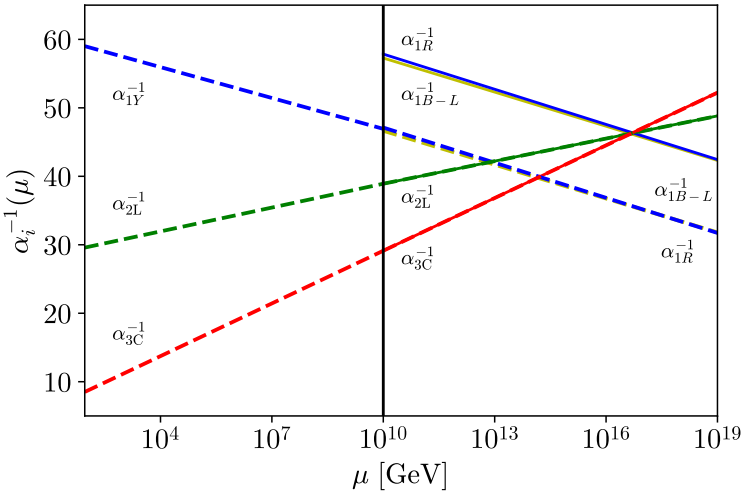

Figure 3.3: The running of the gauge couplings when $\mathcal{G}_{3211}$ is broken to the SM gauge group. In this plot, everything is to one-loop order. The plot also shows, as a vertical line, the intermediate scale M_{I} where $\mathcal{G}_{3211}$ is broken to the $\mathcal{G}_{\mathrm{SM}}$. The dashed lines are without kinetic mixing effects, while the solid lines are with kinetic mixing effects. Here, we have chosen $M_{\mathrm{I}} = 10^{10}$ GeV, $x = 0.99$, and $y = 0.19$. The value of y is only applicable for the cases with mixing.

However, that is quite misleading when considering a larger GUT as part of the picture. The matching conditions at M_{GUT} are not affected by any of the aforementioned effects resulting from going from a gauge group with multiple Abelian factors to one with fewer, but we must consider what happens to the extra off-diagonal term $\tilde{g}$. When breaking SO(10) to $\mathcal{G}_{3211}$, a linear combination of the 45 generators gives the generator corresponding to $\mathrm{U}(1)_R$, while another gives the generator corresponding to $\mathrm{U}(1)_{B-L}$. Thus, no mixing term appears as a direct result of the symmetry breaking. Rather, it becomes nonzero at lower energies as a result of the renormalization group running. Therefore, when later running the couplings from lower energies and up, the extra constraint $\tilde{g} = 0$ must be imposed at M_{GUT} [62, 63]. The complete matching conditions then become

$$\begin{cases} \alpha_{1B-L}^{-1}(M_{\mathrm{GUT}}) = \alpha_{1R}^{-1}(M_{\mathrm{GUT}}) \\ \alpha_{1R}^{-1}(M_{\mathrm{GUT}}) = \alpha_{2\mathrm{L}}^{-1}(M_{\mathrm{GUT}}) \\ \alpha_{2\mathrm{L}}^{-1}(M_{\mathrm{GUT}}) = \alpha_{3\mathrm{C}}^{-1}(M_{\mathrm{GUT}}) \\ \tilde{g}(M_{\mathrm{GUT}}) = 0 \end{cases} . \tag{3.57}$$

As a result, not all combinations of x and y are allowed for a certain choice of the two scales M_{I} and M_{GUT}. Keeping the values of x and M_{I} from the plot in figure 3.3, but modifying y so that $\tilde{g} = 0$ at a value chosen as $M_{\mathrm{GUT}} = 10^{16}\,\mathrm{GeV}$, we instead get the plot in figure 3.4. Note that α^{-1}_{1B-L} is slightly covered in the plot, due to x being so close to one. It is also shown how the off-diagonal term $\tilde{g}$ behaves. We see that the addition of kinetic mixing is not enough to achieve unification without threshold effects, but it can still reduce the size of the corrections needed to save the model, as it can move the couplings closer to each other. This will be explored further in Ch. 5.

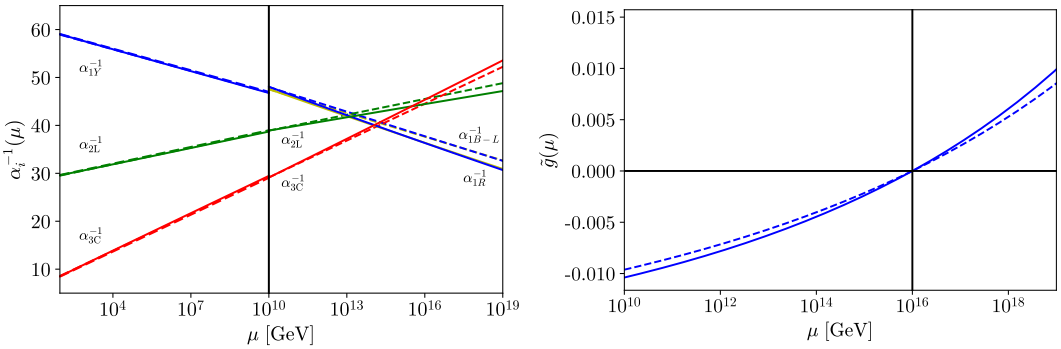

(a) **(b)**

Figure 3.4: **(a)** The running of the gauge couplings in the group $\mathcal{G}_{3211}$, including the effects of kinetic mixing, to one-loop order (dashed) and two-loop order (solid). The plot also shows, as a vertical line, the intermediate scale M_{I} where $\mathcal{G}_{3211}$ is broken to the $\mathcal{G}_{\mathrm{SM}}$. Here, $M_{\mathrm{I}} = 10^{10}\,\mathrm{GeV}$ and $x = 0.99$, while $y = 0.019$ at one-loop order and $y = 0.020$ at two-loop order. **(b)** The running of the off-diagonal coupling $\tilde{g}$ from $M_{\mathrm{I}} = 10^{10}\,\mathrm{GeV}$, where $x = 0.99$, $y = 0.019$ at one-loop order, and $y = 0.020$ at two-loop order are chosen so that $\tilde{g} = 0$ at $\mu = 10^{16}\,\mathrm{GeV}$.

Chapter 4

Threshold effects

As noted in the previous chapter, it is not possible to achieve unification at tree-level matching in either of the two discussed models. However, at higher orders, extra correction terms appear in the matching conditions when symmetries are broken, which can allow us to achieve unification again. Such corrections are the focus of this chapter. How the matching conditions change was discussed in Ch. 2, and here we will apply that to the two models. In order to do that, we must also choose the mass scales of the fields that appear from the decomposition of the GUT fields, when breaking the GUT symmetry. This will follow the same idea as in the last chapter; that the model should be as minimalistic as possible. Thus, only fields that are needed to reproduce the SM will be placed at lower scales. Also, it will be assumed that the parameters η_i are independent of each other. It is possible, depending on the scalar potential, that there are correlations between scalar masses.

4.1 Threshold corrections in model 1

Let us first look at how the addition of threshold corrections alters the $\mathcal{G}_{51}$ model. First of all, we need to know which fields live at which scales, in order to calculate the different coefficients in the expression for the threshold corrections. From a table of group representation decompositions [64], we can see which fields are produced from breaking the GUT symmetry. Then, we can follow the spirit of the extended survival hypothesis, and only place the necessary fields at M_{I}, while the rest are put at M_{GUT}. This is illustrated in table 4.1, where it is shown which fields lie at which scales, when following the breaking chain of model 1.

Knowing the representation of each field that is named in the table, we can insert the proper factors in Eq. (2.97), in order to calculate λ_n^m. For the threshold corrections at M_{GUT}, we find that

$$\begin{aligned} \lambda_{1X}^{10} &= 8 + \eta_{S_1} + 8\eta_{S_2} + 8\eta_{S_3} + 27\eta_{S_5} + 18\eta_{S_6} + \eta_{S_7} + 5\eta_{S_8}\,, \\ \lambda_5^{10} &= 3 + \eta_{S_1} + 3\eta_{S_2} + 3\eta_{S_3} + 7\eta_{S_5} + 3\eta_{S_6} + \eta_{S_7}\,. \end{aligned} \tag{4.1}$$

Group:	SO(10)	$\mathcal{G}_{51}$	$\mathcal{G}_{51}$	$\mathcal{G}_{\rm SM}$
Scale:	$> M_{\rm GUT}$	$M_{\rm GUT}$	$M_{\rm I}$	$M_{\rm I}$
	$\mathbf{10}_{\rm H}$	$S_1(\overline{\mathbf{5}})_2$	$\mathbf{5}_{-2}$	$\phi(\mathbf{3},\mathbf{1})_{-1/3}$
	$\mathbf{45}_{\rm H}$	$S_2(\mathbf{10})_{-4}$, $S_3(\overline{\mathbf{10}})_4$,	$\mathbf{24}_0$	$A_1(\mathbf{8},\mathbf{1})_0$, $A_2(\mathbf{3},\mathbf{2})_{1/6}$,
		$S_4(\mathbf{1})_0$		$A_3(\overline{\mathbf{3}},\mathbf{2})_{-1/6}$, $A_4(\mathbf{1},\mathbf{3})_0$,
				$A_5(\mathbf{1},\mathbf{1})_0$
	$\overline{\mathbf{126}}_{\rm H}$	$S_5(\overline{\mathbf{15}})_{-6}$, $S_6(\mathbf{10})_6$,	$\overline{\mathbf{50}}_2$,	$R_1(\mathbf{8},\mathbf{2})_{1/2}$, $R_2(\overline{\mathbf{6}},\mathbf{3})_{1/3}$,
		$S_7(\overline{\mathbf{5}})_2$, $S_8(\mathbf{1})_{10}$		$R_3(\mathbf{6},\mathbf{1})_{2/3}$, $R_4(\mathbf{3},\mathbf{2})_{1/6}$,
				$R_5(\overline{\mathbf{3}},\mathbf{1})_{1/3}$, $R_6(\mathbf{1},\mathbf{1})_0$
			$\mathbf{45}_{-2}$	$T_1(\mathbf{8},\mathbf{2})_{-1/2}$, $T_2(\mathbf{6},\mathbf{1})_{-1/3}$,
				$T_3(\mathbf{3},\mathbf{3})_{-1/3}$, $T_4(\overline{\mathbf{3}},\mathbf{2})_{-1/6}$,
				$T_5(\mathbf{3},\mathbf{1})_{-1/3}$, $T_6(\overline{\mathbf{3}},\mathbf{1})_{-2/3}$,
				$T_7(\mathbf{1},\mathbf{2})_{-1/2}$
	$\mathbf{45}$	$\mathbf{10}_{-4}$, $\overline{\mathbf{10}}_4$, $\mathbf{1}_0$	$\mathbf{24}_0$	$(\mathbf{3},\mathbf{2})_{1/6}$, $(\overline{\mathbf{3}},\mathbf{2})_{-1/6}$

Table 4.1: The fields at different scales when having $\mathcal{G}_{51}$ as the intermediate symmetry between SO(10) and $\mathcal{G}_{\rm SM}$.

For the threshold corrections at $M_{\rm I}$, we instead find that

$$\begin{aligned}
\lambda_{1Y}^{51} &= \frac{1}{5} + \frac{2}{5}\eta_\phi + \frac{1}{5}\eta_{A_2} + \frac{1}{5}\eta_{A_3} + \frac{24}{5}\eta_{R_1} + \frac{12}{5}\eta_{R_2} + \frac{16}{5}\eta_{R_3} + \frac{1}{5}\eta_{R_4} + \frac{2}{5}\eta_{R_5} \\
&\quad + \frac{24}{5}\eta_{T_1} + \frac{4}{5}\eta_{T_2} + \frac{6}{5}\eta_{T_3} + \frac{1}{5}\eta_{T_4} + \frac{2}{5}\eta_{T_5} + \frac{8}{5}\eta_{T_6} + \frac{3}{5}\eta_{T_7}\,, \\
\lambda_{2L}^{51} &= 3 + 3\eta_{A_2} + 3\eta_{A_3} + 4\eta_{A_4} + 8\eta_{R_1} + 24\eta_{R_2} + 3\eta_{R_4} \\
&\quad + 8\eta_{T_1} + 12\eta_{T_3} + 3\eta_{T_4} + \eta_{T_7}\,, \\
\lambda_{3C}^{51} &= 2 + \eta_\phi + 6\eta_{A_1} + 2\eta_{A_2} + 2\eta_{A_3} + 12\eta_{R_1} + 15\eta_{R_2} + 5\eta_{R_3} + 2\eta_{R_4} + \eta_{R_5} \\
&\quad + 12\eta_{T_1} + 5\eta_{T_2} + 3\eta_{T_3} + 2\eta_{T_4} + \eta_{T_5} + \eta_{T_6}\,.
\end{aligned} \tag{4.2}$$

Now we can look at how the matching conditions are modified by the addition of these corrections, by using Eq. (2.94). At the intermediate scale $M_{\rm I}$, we get the matching conditions

$$\begin{cases}
\alpha_{1X}^{-1}(M_{\rm I}) = \frac{1}{24}\left(25\alpha_{1Y}^{-1}(M_{\rm I}) - \alpha_{2L}^{-1}(M_{\rm I}) + \frac{1}{12\pi}\left(25\lambda_{1Y}^{51} - \lambda_{2L}^{51}\right)\right) \\
\alpha_5^{-1}(M_{\rm I}) = \alpha_{2L}^{-1}(M_{\rm I}) + \frac{\lambda_{2L}^{51}}{12\pi} \\
\alpha_5^{-1}(M_{\rm I}) = \alpha_{3C}^{-1}(M_{\rm I}) + \frac{\lambda_{3C}^{51}}{12\pi}
\end{cases}. \tag{4.3}$$

Just like in the case without any corrections, $\alpha_5^{-1}(M_{\rm I})$ can be eliminated from the two last equations of this system. This results in

$$\begin{cases} \alpha_{1X}^{-1}(M_{\rm I}) = \frac{1}{24}\left(25\alpha_{1Y}^{-1}(M_{\rm I}) - \alpha_{2\rm L}^{-1}(M_{\rm I}) + \frac{1}{12\pi}\left(25\lambda_{1Y}^{51} - \lambda_{2\rm L}^{51}\right)\right) \\ \alpha_{3\rm C}^{-1}(M_{\rm I}) - \alpha_{2\rm L}^{-1}(M_{\rm I}) + \frac{1}{12\pi}(\lambda_{3\rm C}^{51} - \lambda_{2\rm L}^{51}) = 0 \end{cases}, \tag{4.4}$$

which again shows that $M_{\rm I}$ can be found from just the second equation, thus only depending on the difference between the two corrections $\lambda_{2\rm L}^{51}$ and $\lambda_{3\rm C}^{51}$. At the unification scale $M_{\rm GUT}$, we instead get the system

$$\begin{cases} \alpha_{10}^{-1}(M_{\rm GUT}) = \alpha_{1X}^{-1}(M_{\rm GUT}) + \frac{\lambda_{1X}^{10}}{12\pi} \\ \alpha_{10}^{-1}(M_{\rm GUT}) = \alpha_5^{-1}(M_{\rm GUT}) + \frac{\lambda_5^{10}}{12\pi} \end{cases}, \tag{4.5}$$

which can simplified to the single equation

$$\alpha_5^{-1}(M_{\rm GUT}) - \alpha_{1X}^{-1}(M_{\rm GUT}) + \frac{1}{12\pi}(\lambda_5^{10} - \lambda_{1X}^{10}) = 0\,. \tag{4.6}$$

The interesting part that makes this model stand out from other ones, is that the two variables $M_{\rm I}$ and $M_{\rm GUT}$ again are somewhat decoupled in this system of equations. What this means is that $M_{\rm I}$ can be found separately from $M_{\rm GUT}$, just given the threshold corrections at the intermediate scale. Then, that value along with the threshold corrections at the unification scale can be used to find the corresponding value of $M_{\rm GUT}$.

We can also note that analytical expressions again can be found for each scale, in the one-loop case. Inserting the known one-loop SM solutions into Eq. (4.4), we get

$$\frac{19}{12\pi}\ln\left(\frac{M_{\rm I}}{M_{\rm Z}}\right) + \alpha_{2\rm L}^{-1}(M_{\rm Z}) + \frac{\lambda_{2\rm L}^{51}}{12\pi} = \frac{7}{2\pi}\ln\left(\frac{M_{\rm I}}{M_{\rm Z}}\right) + \alpha_{3\rm C}^{-1}(M_{\rm Z}) + \frac{\lambda_{3\rm C}^{51}}{12\pi}\,, \tag{4.7}$$

which gives

$$M_{\rm I} = M_{\rm Z}\exp\left\{\frac{12\pi}{23}\left[\alpha_{2\rm L}^{-1}(M_{\rm Z}) - \alpha_{3\rm C}^{-1}(M_{\rm Z}) + \frac{1}{12\pi}\left(\lambda_{2\rm L}^{51} - \lambda_{3\rm C}^{51}\right)\right]\right\}. \tag{4.8}$$

Using this, along with the other initial values at $M_{\rm I}$, Eq. (4.6) gives the unification scale. This is done by inserting the known one-loop solutions for the $\mathcal{G}_{51}$ couplings, giving

$$\begin{aligned} M_{\rm GUT} = M_{\rm I}\exp\Bigg\{\frac{\pi}{5}\Bigg[&\frac{\lambda_{1X}^{10} - \lambda_5^{10}}{12\pi} + \frac{25}{24}\Bigg(-\frac{109}{30\pi}\ln\left(\frac{M_{\rm I}}{M_{\rm Z}}\right) \\ &+\alpha_{1Y}^{-1}(M_{\rm Z}) - \alpha_{2\rm L}^{-1}(M_{\rm Z}) + \frac{\lambda_{1Y}^{51} - \lambda_{2\rm L}^{51}}{12\pi}\Bigg)\Bigg]\Bigg\}\,. \end{aligned} \tag{4.9}$$

The system of equations can also be solved for the two-loop case, but must then instead be done so numerically, as will be done in the next chapter.

4.2 Threshold corrections in model 2

We can now also examine how threshold corrections change the model based on the intermediate gauge group $\mathcal{G}_{3211}$. Following the same procedure as before when deciding which fields go at which scale, the fields at different scales are shown in table 4.2.

Group:	SO(10)	$\mathcal{G}_{3211}$	$\mathcal{G}_{3211}$	$\mathcal{G}_{\rm SM}$
Scale:	$> M_{\rm GUT}$	$M_{\rm GUT}$	$M_{\rm I}$	$M_{\rm I}$
	$\mathbf{10}_{\rm H}$	$S_1(\mathbf{3},\mathbf{1})_{0,-\frac{2}{3}}$, $S_2(\overline{\mathbf{3}},\mathbf{1})_{0,\frac{2}{3}}$, $S_3(\mathbf{1},\mathbf{2})_{\frac{1}{2},0}$	$(\mathbf{1},\mathbf{2})_{-\frac{1}{2},0}$	$\phi(\mathbf{1},\mathbf{2})_{1/2}$
	$\mathbf{45}_{\rm H}$	$S_4(\mathbf{3},\mathbf{2})_{\frac{1}{2},-\frac{2}{3}}$, $S_5(\mathbf{3},\mathbf{2})_{-\frac{1}{2},-\frac{2}{3}}$, $S_6(\overline{\mathbf{3}},\mathbf{2})_{\frac{1}{2},\frac{2}{3}}$, $S_7(\overline{\mathbf{3}},\mathbf{2})_{-\frac{1}{2},\frac{2}{3}}$, $S_8(\mathbf{8},\mathbf{1})_{0,0}$, $S_9(\mathbf{3},\mathbf{1})_{0,\frac{4}{3}}$, $S_{10}(\overline{\mathbf{3}},\mathbf{1})_{0,-\frac{4}{3}}$, $S_{11}(\mathbf{1},\mathbf{3})_{0,0}$, $S_{12}(\mathbf{1},\mathbf{1})_{1,0}$, $S_{13}(\mathbf{1},\mathbf{1})_{0,0}$, $S_{14}(\mathbf{1},\mathbf{1})_{-1,0}$	$(\mathbf{1},\mathbf{1})_{0,0}$	$(\mathbf{1},\mathbf{1})_0$
	$\overline{\mathbf{126}}_{\rm H}$	$R_1(\mathbf{8},\mathbf{2})_{\frac{1}{2},0}$, $R_2(\mathbf{8},\mathbf{2})_{-\frac{1}{2},0}$, $R_3(\mathbf{1},\mathbf{2})_{\frac{1}{2},0}$, $R_4(\mathbf{3},\mathbf{2})_{\frac{1}{2},\frac{4}{3}}$, $R_5(\mathbf{3},\mathbf{2})_{-\frac{1}{2},\frac{4}{3}}$, $R_6(\overline{\mathbf{3}},\mathbf{2})_{\frac{1}{2},-\frac{4}{3}}$, $R_7(\overline{\mathbf{3}},\mathbf{2})_{-\frac{1}{2},-\frac{4}{3}}$, $R_8(\mathbf{6},\mathbf{1})_{1,-\frac{2}{3}}$, $R_9(\mathbf{6},\mathbf{1})_{0,-\frac{2}{3}}$, $R_{10}(\mathbf{6},\mathbf{1})_{-1,-\frac{2}{3}}$, $R_{11}(\overline{\mathbf{3}},\mathbf{1})_{1,\frac{2}{3}}$, $R_{12}(\overline{\mathbf{3}},\mathbf{1})_{0,\frac{2}{3}}$, $R_{13}(\overline{\mathbf{3}},\mathbf{1})_{-1,\frac{2}{3}}$, $R_{14}(\mathbf{1},\mathbf{1})_{0,2}$, $R_{15}(\mathbf{1},\mathbf{1})_{-1,2}$	$(\mathbf{1},\mathbf{2})_{-\frac{1}{2},0}$, $(\mathbf{1},\mathbf{1})_{1,2}$	$(\mathbf{1},\mathbf{1})_0$
	$\mathbf{210}_{\rm H}$	$T_1(\mathbf{8},\mathbf{3})_{0,0}$, $T_2(\mathbf{3},\mathbf{3})_{0,\frac{4}{3}}$, $T_3(\overline{\mathbf{3}},\mathbf{3})_{0,-\frac{4}{3}}$, $T_4(\mathbf{1},\mathbf{3})_{0,0}$, $T_5(\mathbf{8},\mathbf{1})_{1,0}$, $T_6(\mathbf{8},\mathbf{1})_{0,0}$, $T_7(\mathbf{8},\mathbf{1})_{-1,0}$, $T_8(\mathbf{3},\mathbf{1})_{1,\frac{4}{3}}$, $T_9(\mathbf{3},\mathbf{1})_{0,\frac{4}{3}}$, $T_{10}(\mathbf{3},\mathbf{1})_{-1,\frac{4}{3}}$, $T_{11}(\overline{\mathbf{3}},\mathbf{1})_{1,-\frac{4}{3}}$, $T_{12}(\overline{\mathbf{3}},\mathbf{1})_{0,-\frac{4}{3}}$, $T_{13}(\overline{\mathbf{3}},\mathbf{1})_{-1,-\frac{4}{3}}$, $T_{14}(\mathbf{1},\mathbf{1})_{1,0}$,	$(\mathbf{1},\mathbf{1})_{0,0}$, $(\mathbf{1},\mathbf{1})_{0,0}$	$(\mathbf{1},\mathbf{1})_0$

	$T_{15}(\mathbf{1},\mathbf{1})_{0,0}$, $T_{16}(\mathbf{1},\mathbf{1})_{-1,0}$, $T_{17}(\overline{\mathbf{6}},\mathbf{2})_{\frac{1}{2},\frac{2}{3}}$, $T_{18}(\overline{\mathbf{6}},\mathbf{2})_{-\frac{1}{2},\frac{2}{3}}$, $T_{19}(\mathbf{3},\mathbf{2})_{\frac{1}{2},-\frac{2}{3}}$, $T_{20}(\mathbf{3},\mathbf{2})_{-\frac{1}{2},-\frac{2}{3}}$, $T_{21}(\mathbf{6},\mathbf{2})_{\frac{1}{2},-\frac{2}{3}}$, $T_{22}(\mathbf{6},\mathbf{2})_{-\frac{1}{2},-\frac{2}{3}}$, $T_{23}(\overline{\mathbf{3}},\mathbf{2})_{\frac{1}{2},\frac{2}{3}}$, $T_{24}(\overline{\mathbf{3}},\mathbf{2})_{-\frac{1}{2},\frac{2}{3}}$, $T_{25}(\mathbf{1},\mathbf{2})_{\frac{1}{2},-2}$, $T_{26}(\mathbf{1},\mathbf{2})_{-\frac{1}{2},-2}$, $T_{27}(\mathbf{1},\mathbf{2})_{\frac{1}{2},2}$, $T_{28}(\mathbf{1},\mathbf{2})_{-\frac{1}{2},2}$, $T_{29}(\mathbf{3},\mathbf{2})_{\frac{1}{2},-\frac{2}{3}}$, $T_{30}(\mathbf{3},\mathbf{2})_{-\frac{1}{2},-\frac{2}{3}}$, $T_{31}(\overline{\mathbf{3}},\mathbf{2})_{\frac{1}{2},\frac{2}{3}}$, $T_{32}(\overline{\mathbf{3}},\mathbf{2})_{-\frac{1}{2},\frac{2}{3}}$, $T_{33}(\mathbf{8},\mathbf{1})_{0,0}$, $T_{34}(\mathbf{3},\mathbf{1})_{0,\frac{4}{3}}$, $T_{35}(\overline{\mathbf{3}},\mathbf{1})_{0,-\frac{4}{3}}$, $T_{36}(\mathbf{1},\mathbf{1})_{0,0}$		
45	$(\mathbf{3},\mathbf{2})_{\frac{1}{2},-\frac{2}{3}}$, $(\mathbf{3},\mathbf{2})_{-\frac{1}{2},-\frac{2}{3}}$, $(\overline{\mathbf{3}},\mathbf{2})_{\frac{1}{2},\frac{2}{3}}$, $(\overline{\mathbf{3}},\mathbf{2})_{-\frac{1}{2},\frac{2}{3}}$, $(\mathbf{3},\mathbf{1})_{0,\frac{4}{3}}$, $(\overline{\mathbf{3}},\mathbf{1})_{0,-\frac{4}{3}}$, $(\mathbf{1},\mathbf{1})_{1,0}$, $(\mathbf{1},\mathbf{1})_{0,0}$, $(\mathbf{1},\mathbf{1})_{-1,0}$	$(\mathbf{8},\mathbf{1})_{0,0}$, $(\mathbf{1},\mathbf{3})_{0,0}$, $(\mathbf{1},\mathbf{1})_{0,0}$	$(\mathbf{8},\mathbf{1})_0$, $(\mathbf{1},\mathbf{3})_0$, $(\mathbf{1},\mathbf{1})_0$

Table 4.2: The fields at different scales when having $\mathcal{G}_{3211}$ as the intermediate symmetry between SO(10) and $\mathcal{G}_{\rm SM}$.

One interesting property of this model that can be seen, which is important for the later numerical analysis, is that the possible sizes of the threshold effects at $M_{\rm GUT}$ far outweigh those at $M_{\rm I}$, when the different η_i are in the same range. This follows from that the gauge group $\mathcal{G}_{3211}$ is very similar to the SM gauge group $\mathcal{G}_{\rm SM}$, in the sense that only an extra Abelian factor U(1) separates them. Therefore, the only $\mathcal{G}_{3211}$ fields that need to be placed at $M_{\rm I}$ in order to reproduce the SM correctly after symmetry breaking are SM representations with an extra Abelian charge, which do not break into extra representations with masses around $M_{\rm I}$. The effect of this can be seen when using Eq. (2.97) to compute the expressions for the threshold corrections. At $M_{\rm I}$, we just get

$$\begin{aligned} \lambda_{3C}^{3211} &= 3\,, \\ \lambda_{2L}^{3211} &= 2+\eta_\phi\,, \\ \lambda_{1Y}^{3211} &= \frac{3}{5}\eta_\phi\,. \end{aligned} \tag{4.10}$$

At $M_{\rm GUT}$, we instead find that

$$\begin{aligned}
\lambda^{10}_{3\rm C} &= 5 + \eta_{S_1} + \eta_{S_2} + 2\eta_{S_4} + 2\eta_{S_5} + 2\eta_{S_6} + 2\eta_{S_7} + 6\eta_{S_8} + \eta_{S_9} + \eta_{S_{10}} \\
&\quad + 12\eta_{R_1} + 12\eta_{R_2} + 2\eta_{R_4} + 2\eta_{R_5} + 2\eta_{R_6} + 2\eta_{R_7} \\
&\quad + 5\eta_{R_8} + 5\eta_{R_9} + 5\eta_{R_{10}} + \eta_{R_{11}} + \eta_{R_{12}} + \eta_{R_{13}} \\
&\quad + 18\eta_{T_1} + 3\eta_{T_2} + 3\eta_{T_3} + 6\eta_{T_5} + 6\eta_{T_6} + 6\eta_{T_7} + \eta_{T_8} + \eta_{T_9} + \eta_{T_{10}} \\
&\quad + \eta_{T_{11}} + \eta_{T_{12}} + \eta_{T_{13}} + 10\eta_{T_{17}} + 10\eta_{T_{18}} + 2\eta_{T_{19}} + 2\eta_{T_{20}} + 10\eta_{T_{21}} + 10\eta_{T_{22}} \\
&\quad + 2\eta_{T_{23}} + 2\eta_{T_{24}} + 2\eta_{T_{29}} + 2\eta_{T_{30}} + 2\eta_{T_{31}} + 2\eta_{T_{32}} + 6\eta_{T_{33}} + \eta_{T_{34}} + \eta_{T_{35}} \,, \\
\lambda^{10}_{2\rm L} &= 6 + \eta_{S_3} + 3\eta_{S_4} + 3\eta_{S_5} + 3\eta_{S_6} + 3\eta_{S_7} + 4\eta_{S_{11}} \\
&\quad + 8\eta_{R_1} + 8\eta_{R_2} + \eta_{R_3} + 3\eta_{R_4} + 3\eta_{R_5} + 3\eta_{R_6} + 3\eta_{R_7} \\
&\quad + 32\eta_{T_1} + 12\eta_{T_2} + 12\eta_{T_3} + 4\eta_{T_4} + 6\eta_{T_{17}} + 6\eta_{T_{18}} + 3\eta_{T_{19}} + 3\eta_{T_{20}} \\
&\quad + 6\eta_{T_{21}} + 6\eta_{T_{22}} + 3\eta_{T_{23}} + 3\eta_{T_{24}} + \eta_{T_{25}} + \eta_{T_{26}} + \eta_{T_{27}} + \eta_{T_{28}} \\
&\quad + 3\eta_{T_{29}} + 3\eta_{T_{30}} + 3\eta_{T_{31}} + 3\eta_{T_{32}} \,, \\
\lambda^{10}_{1R} &= 8 + \eta_{S_3} + 3\eta_{S_4} + 3\eta_{S_5} + 3\eta_{S_6} + 3\eta_{S_7} + 2\eta_{S_{12}} + 2\eta_{S_{14}} \\
&\quad + 8\eta_{R_1} + 8\eta_{R_2} + \eta_{R_3} + 3\eta_{R_4} + 3\eta_{R_5} + 3\eta_{R_6} + 3\eta_{R_7} \\
&\quad + 12\eta_{R_8} + 12\eta_{R_{10}} + 6\eta_{R_{11}} + 6\eta_{R_{13}} + 2\eta_{R_{15}} \\
&\quad + 16\eta_{T_6} + 16\eta_{T_7} + 6\eta_{T_8} + 6\eta_{T_{10}} + 6\eta_{T_{11}} + 6\eta_{T_{13}} + 2\eta_{T_{14}} + 2\eta_{T_{16}} \\
&\quad + 6\eta_{T_{17}} + 6\eta_{T_{18}} + 3\eta_{T_{19}} + 3\eta_{T_{20}} + 6\eta_{T_{21}} + 6\eta_{T_{22}} + 3\eta_{T_{23}} + 3\eta_{T_{24}} \\
&\quad + \eta_{T_{25}} + \eta_{T_{26}} + \eta_{T_{27}} + \eta_{T_{28}} + 3\eta_{T_{29}} + 3\eta_{T_{30}} + 3\eta_{T_{31}} + 3\eta_{T_{32}} \,, \\
\lambda^{10}_{1B-L} &= 8 + \eta_{S_1} + \eta_{S_2} + 2\eta_{S_4} + 2\eta_{S_5} + 2\eta_{S_6} + 2\eta_{S_7} + 4\eta_{S_9} + 4\eta_{S_{10}} \\
&\quad + 8\eta_{R_4} + 8\eta_{R_5} + 8\eta_{R_6} + 8\eta_{R_7} \\
&\quad + 2\eta_{R_8} + 2\eta_{R_9} + 2\eta_{R_{10}} + \eta_{R_{11}} + \eta_{R_{12}} + \eta_{R_{13}} + 8\eta_{R_{14}} + 8\eta_{R_{15}} \\
&\quad + 12\eta_{T_2} + 12\eta_{T_3} + 4\eta_{T_8} + 4\eta_{T_9} + 4\eta_{T_{10}} + 4\eta_{T_{11}} + 4\eta_{T_{12}} + 4\eta_{T_{13}} \\
&\quad + 4\eta_{T_{17}} + 4\eta_{T_{18}} + 2\eta_{T_{19}} + 2\eta_{T_{20}} + 4\eta_{T_{21}} + 4\eta_{T_{22}} + 2\eta_{T_{23}} + 2\eta_{T_{24}} \\
&\quad + 6\eta_{T_{25}} + 6\eta_{T_{26}} + 6\eta_{T_{27}} + 6\eta_{T_{28}} + 2\eta_{T_{29}} + 2\eta_{T_{30}} + 2\eta_{T_{31}} + 2\eta_{T_{32}} \\
&\quad + 4\eta_{T_{34}} + 4\eta_{T_{35}} \,.
\end{aligned} \tag{4.11}$$

With these threshold effects, the matching conditions at $M_{\rm I}$, which give the initial values for the $\mathcal{G}_{3211}$ couplings, become

$$\begin{cases}
\alpha^{-1}_{1B-L}\left(M_1\right) = x\left(\frac{2}{5}x + \frac{3}{5}\right)^{-1}\left(\alpha^{-1}_{1Y}\left(M_{\rm I}\right) + \frac{\lambda^{3211}_{1Y}}{12\pi}\right) \\
\alpha^{-1}_{1R}\left(M_{\rm I}\right) = \left(\frac{2}{5}x + \frac{3}{5}\right)^{-1}\left(\alpha^{-1}_{1Y}\left(M_{\rm I}\right) + \frac{\lambda^{3211}_{1Y}}{12\pi}\right) \\
\alpha^{-1}_{2\rm L}(M_{\rm I}) = \alpha^{-1}_{2\rm L}(M_{\rm I}) + \frac{\lambda^{3211}_{2\rm L}}{12\pi} \\
\alpha^{-1}_{3\rm C}(M_{\rm I}) = \alpha^{-1}_{3\rm C}(M_{\rm I}) + \frac{\lambda^{3211}_{3\rm C}}{12\pi}
\end{cases} . \tag{4.12}$$

Similarly, by adding corrections, the matching conditions at $M_{\rm GUT}$ become

$$\begin{cases} \alpha_{10}^{-1}(M_{\rm GUT}) = \alpha_{1B-L}^{-1}(M_{\rm GUT}) + \frac{\lambda_{1B-L}^{10}}{12\pi} \\ \alpha_{10}^{-1}(M_{\rm GUT}) = \alpha_{1R}^{-1}(M_{\rm GUT}) + \frac{\lambda_{1R}^{10}}{12\pi} \\ \alpha_{10}^{-1}(M_{\rm GUT}) = \alpha_{2\rm L}^{-1}(M_{\rm GUT}) + \frac{\lambda_{2\rm L}^{10}}{12\pi} \\ \alpha_{10}^{-1}(M_{\rm GUT}) = \alpha_{3\rm C}^{-1}(M_{\rm GUT}) + \frac{\lambda_{3\rm C}^{10}}{12\pi} \end{cases}, \tag{4.13}$$

where the GUT coupling $\alpha_{10}^{-1}(M_{\rm GUT})$ again can be eliminated, leaving us with the three equations

$$\begin{cases} \alpha_{1B-L}^{-1}(M_{\rm GUT}) - \alpha_{1R}^{-1}(M_{\rm GUT}) + \frac{1}{12\pi}(\lambda_{1B-L}^{10} - \lambda_{1R}^{10}) = 0 \\ \alpha_{1R}^{-1}(M_{\rm GUT}) - \alpha_{2\rm L}^{-1}(M_{\rm GUT}) + \frac{1}{12\pi}(\lambda_{1R}^{10} - \lambda_{2\rm L}^{10}) = 0 \\ \alpha_{2\rm L}^{-1}(M_{\rm GUT}) - \alpha_{3\rm C}^{-1}(M_{\rm GUT}) + \frac{1}{12\pi}(\lambda_{2\rm L}^{10} - \lambda_{3\rm C}^{10}) = 0 \end{cases}. \tag{4.14}$$

As discussed in section 2.6, the threshold corrections take the same form when also considering kinetic mixing in this model. The only thing that must be changed is then the original matching conditions. Adding corrections to the matching conditions at $M_{\rm I}$ from Ch. 3, we get

$$\begin{cases} \alpha_{1B-L}^{-1}(M_{\rm I}) = x\left(\frac{2}{5}x + \frac{3}{5} - \frac{\sqrt{6}}{5}y(x+\sqrt{x})\right)^{-1}\left(\alpha_{1Y}^{-1}(M_{\rm I}) + \frac{\lambda_{1Y}^{3211}}{12\pi}\right) \\ \alpha_{1R}^{-1}(M_{\rm I}) = \left(\frac{2}{5}x + \frac{3}{5} - \frac{\sqrt{6}}{5}y(x+\sqrt{x})\right)^{-1}\left(\alpha_{1Y}^{-1}(M_{\rm I}) + \frac{\lambda_{1Y}^{3211}}{12\pi}\right) \\ \tilde{\alpha}^{-1}(M_{\rm I}) = \frac{1}{y^2}\left(\frac{2}{5}x + \frac{3}{5} - \frac{\sqrt{6}}{5}y(x+\sqrt{x})\right)^{-1}\left(\alpha_{1Y}^{-1}(M_{\rm I}) + \frac{\lambda_{1Y}^{3211}}{12\pi}\right) \\ \alpha_{2\rm L}^{-1}(M_{\rm I}) = \alpha_{2\rm L}^{-1}(M_{\rm I}) + \frac{\lambda_{2\rm L}^{3211}}{12\pi} \\ \alpha_{3\rm C}^{-1}(M_{\rm I}) = \alpha_{3\rm C}^{-1}(M_{\rm I}) + \frac{\lambda_{3\rm C}^{3211}}{12\pi} \end{cases}. \tag{4.15}$$

At $M_{\rm GUT}$ we must only add the extra condition $\tilde{g}(M_{\rm GUT}) = 0$ to the ones in Eq. (4.14), since the mixing effects are not seen there. This gives

$$\begin{cases} \alpha_{1B-L}^{-1}(M_{\rm GUT}) - \alpha_{1R}^{-1}(M_{\rm GUT}) + \frac{1}{12\pi}(\lambda_{1B-L}^{10} - \lambda_{1R}^{10}) = 0 \\ \alpha_{1R}^{-1}(M_{\rm GUT}) - \alpha_{2\rm L}^{-1}(M_{\rm GUT}) + \frac{1}{12\pi}(\lambda_{1R}^{10} - \lambda_{2\rm L}^{10}) = 0 \\ \alpha_{2\rm L}^{-1}(M_{\rm GUT}) - \alpha_{3\rm C}^{-1}(M_{\rm GUT}) + \frac{1}{12\pi}(\lambda_{2\rm L}^{10} - \lambda_{3\rm C}^{10}) = 0 \\ \tilde{g}(M_{\rm GUT}) = 0 \end{cases}, \tag{4.16}$$

as the system of equations to be solved.

Chapter 5

Numerical methods and results

Apart from the one-loop cases without kinetic mixing, the renormalization group equations are not analytically solvable, due to the intricate way they are coupled with each other. Therefore, numerical solvers are a must when analyzing the running in these models. Some examples of this have already been seen in the previous sections, where the two-loop running of coupling constants was plotted. However, the numerical calculations will become a bit more involved here. All of the code used for the following numerical analysis is written in `Python 3.7.1`. Some of the results are made by running the scripts locally, while some of the more computationally heavy ones are made using the Beskow supercomputing system. It is a high-performance computing (HPC) cluster, where 48 different cores were used simultaneously.

This chapter will be dedicated to describing the numerical methods used to analyze the effects of threshold corrections in the two models discussed in previous chapters, as well as illustrating the results. Because of the different features of the two models explained in Ch. 3, the numerical approach will differ a bit between the two models. First, the model with $\mathcal{G}_{51}$ as an intermediate symmetry will be treated, followed by the model with $\mathcal{G}_{3211}$ as the intermediate symmetry. As part of the later model, kinetic mixing effects will also be included.

5.1 Numerical analysis of model 1

First of all, we will examine the effects of threshold corrections in the model based on $\mathcal{G}_{51}$. Because of the slight decoupling of the system explained earlier, in the sense that M_{I} can be determined independently, it is quite easy to analyze how the intermediate scale shifts as a result of the corrections. Figure 5.1a shows how M_{I} can be pushed to lower scales, by adding fields with masses near that scale. It can

of course also be pushed to higher scales, by threshold corrections with the opposite sign, but that is of no help when trying to achieve unification. In the plot, it is shown how low M_{I} can be moved, by adding threshold corrections corresponding to $\eta_i \in [-1, 1]$, $\eta_i \in [-2, 2]$, and $\eta_i \in [-3, 3]$. As we noted in Ch. 3, the problem that prevents unification is that the intermediate scale is too high. This leads to $\alpha_{1Y}^{-1} < \alpha_{2\mathrm{L}}^{-1} = \alpha_{3\mathrm{C}}^{-1}$ at the point of symmetry breaking, which in turn results in the $\mathcal{G}_{51}$ couplings immediately starting to move further apart. However, if the threshold corrections are large enough, it is possible to push M_{I} below the scale where the SM couplings cross.

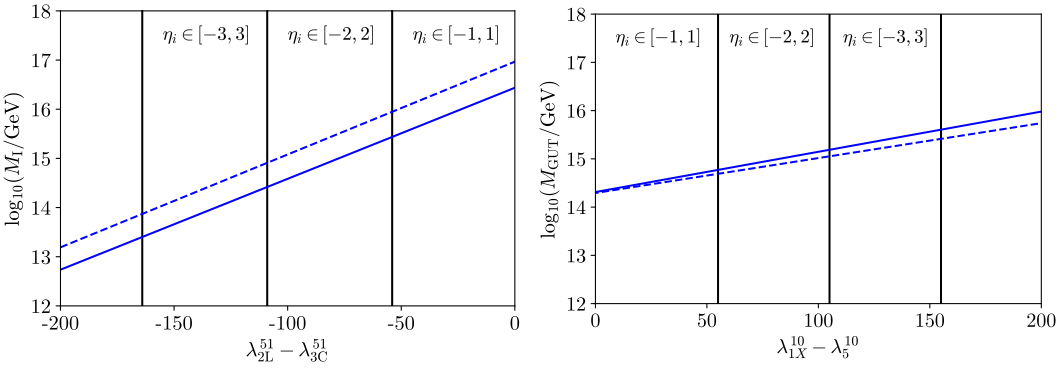

(a) **(b)**

Figure 5.1: The plots illustrate how the two scales can be manipulated semi-independently in this model. In both plots, the different regions separated by vertical lines show which values are reachable with η_i in different intervals. **(a)** How the intermediate scale M_{I} changes depending on the difference $\lambda_{2\mathrm{L}}^{51} - \lambda_{3\mathrm{C}}^{51}$ between threshold corrections around that scale. **(b)** How the unification scale M_{GUT} changes depending on the difference $\lambda_{1X}^{10} - \lambda_{5}^{10}$ between threshold corrections around that scale, given the minimum value of M_{I} from the left plot.

	One-loop	Two-loop
M_{I} [GeV]	7.43×10^{13}	2.52×10^{13}

Table 5.1: The lowest possible values of the intermediate scale M_{I} where $\mathcal{G}_{51}$ is broken to $\mathcal{G}_{\mathrm{SM}}$, with $\eta_i \in [-3, 3]$.

As an example, we can see what happens if we pick the lowest possible M_{I} that can be achieved with $\eta_i \in [-3, 3]$, for both the one- and two-loop cases. These values are shown in table 5.1. Since we then get M_{I} below 10^{14} GeV, it is possible to achieve unification, even without adding corrections at M_{GUT}. However, that would result in the unification scale being quite low, ending up just next to the intermediate scale. We can also add threshold corrections at M_{GUT} as well, in an

attempt to push the unification scale to larger scales. Since Eq. (4.6) only depends on the difference $\lambda_5^{10} - \lambda_{1X}^{10}$, it is easy to perform a similar analysis as for the intermediate scale. In figure 5.1b it is shown how the unification scale varies, given the choice of the lowest possible intermediate scales. Again, the different regions show which scales that can be achieved by having η_i in the different intervals. The maximum values of M_{GUT} that can be achieved, also with $\eta_i \in [-3, 3]$, are shown in table 5.2. Figure 5.2 finally shows the running of the couplings, with these values of the two scales.

	One-loop	Two-loop
M_{GUT} [GeV]	2.60×10^{15}	4.03×10^{15}

Table 5.2: The largest possible values of the unification scale M_{GUT} where SO(10) is broken to $\mathcal{G}_{51}$, with $\eta_i \in [-3, 3]$, and values of M_{I} given in table 5.1.

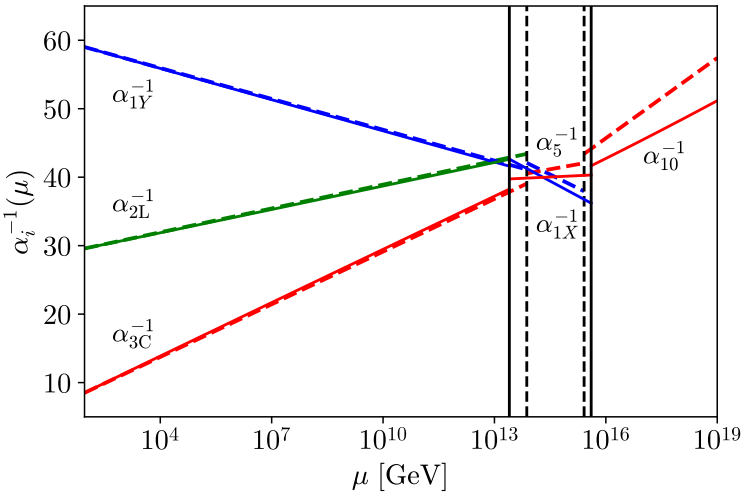

Figure 5.2: An example of unification, allowed by threshold corrections, in the model with $\mathcal{G}_{51}$ as the intermediate symmetry. The running of the coupling constants in $\mathcal{G}_{\mathrm{SM}}$, $\mathcal{G}_{51}$, and SO(10) are shown to one-loop order (dashed) and two-loop order (solid). Here, the threshold corrections are chosen in order to minimize M_{I} and maximize M_{GUT}, with $\eta_i \in [-3, 3]$. These two scales are shown as vertical lines.

From this analysis, we can draw the conclusion that quite few combinations of different η_i actually give physically meaningful solutions to this problem. It is actually not the case that the system is not solvable otherwise; the analytical one-loop expressions in Eqs. (4.8) and (4.9) for M_{I} and M_{GUT} are valid for any threshold corrections, and from numerical error analysis, the two-loop system does

not seem to be unsolvable. What instead happens is that for most choices of threshold corrections, we get solutions in the region where $M_{\mathrm{I}} > M_{\mathrm{GUT}}$, which are not particularly interesting, since that region is unphysical.

We can also perform a random sampling of the parameters η_i, in order to analyze the behavior of the model. Figure 5.3 shows how the two scales vary, when the parameters are sampled in different intervals. This sampling is performed on the Beskow system, with 2×10^9 samplings for the one-loop system and 2×10^6 samplings for the two-loop system. The solid, dashed, and dotted lines correspond to the one-loop solutions when sampling for $\eta_i \in [-3,3]$, $\eta_i \in [-4,4]$, and $\eta_i \in [-5,5]$, respectively. Red regions are instead the two-loop solutions from sampling in the same intervals.

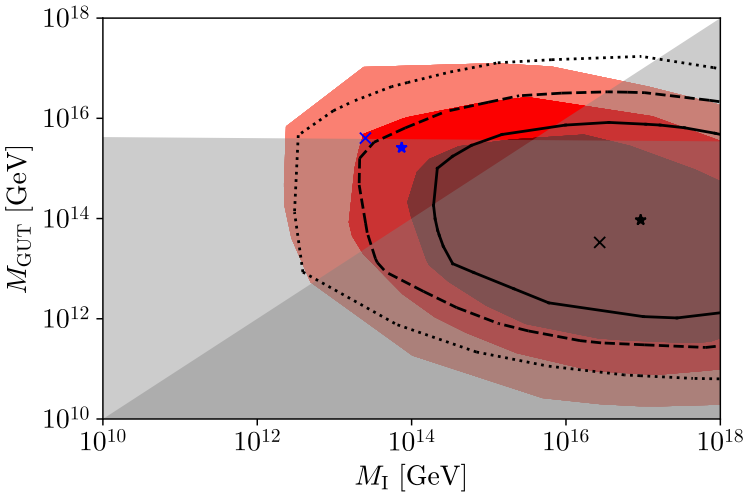

Figure 5.3: The plot shows the values of the intermediate scale M_{I} and the unification scale M_{GUT}, solved from the system of equations in Eq. (4.5), when the parameters η_i are randomly sampled. The solid, dashed, and dotted lines show the one-loop results, while the colored regions show the two-loop results. From smallest to largest, the regions in each of the two cases are given by sampling in the regions $\eta_i \in [-3,3]$, $\eta_i \in [-4,4]$, and $\eta_i \in [-5,5]$. They grey shaded areas are those that are excluded by the proton decay limit (which is almost horizontal), the unphysical limit where $M_{\mathrm{I}} > M_{\mathrm{GUT}}$, or both. The black star (cross) shows the solution without having any threshold effects, to one-loop (two-loop) order, while the blue star (cross) shows the values from tables 5.1 and 5.2.

The different regions are created using the `ConvexHull` method from the `SciPy` package [65]. We see in the figure that, just as expected, most of the solutions are excluded since they are under the line $M_{\mathrm{I}} = M_{\mathrm{GUT}}$. Many values are also ruled out by the horizontal grey region, which is determined by the proton decay limit. The black cross and star correspond to the two solutions that we get without any threshold corrections, and as we noted earlier, they are in the excluded region.

The blue cross and star instead correspond to the solutions that were found when minimizing M_{I} and maximizing M_{GUT}, for $\eta_i \in [-3, 3]$, respectively. Those points, on the other hand, are just on the limit to the allowed region.

5.2 Numerical analysis of model 2

Unfortunately, the system of equations giving the scales for the second model does not behave as nicely as the one for the model 1, where we could always solve for the two scales, given certain threshold corrections. In the model based on $\mathcal{G}_{3211}$, it seems that only very small regions in the parameter space result in a solvable system. This difference between the two models can be seen intuitively from the earlier plots of the couplings, and is the result of having to unify four different couplings at once, instead of just two.

This is where it becomes important that the threshold corrections at M_{I} are negligible in this model, due to almost all fields having masses around M_{GUT}. If we for a moment treat them as negligible, we then see that the system instead can be solved backwards. What this means is that M_{I}, M_{GUT}, and x are treated as input parameters, while the system is solved for the three differences $\lambda^{10}_{1B-L} - \lambda^{10}_{1R}$, $\lambda^{10}_{1R} - \lambda^{10}_{2\mathrm{L}}$, and $\lambda^{10}_{2\mathrm{L}} - \lambda^{10}_{3\mathrm{C}}$. This can always be done, since if the scales are chosen, the differences between the couplings at M_{GUT} can be found. However, this approach then presents us with yet another problem—finding the combination of different η_i which produces these threshold effects. There is obviously an infinite number (or none) of such combinations, since they are solutions to the linear system of equations

$$\begin{cases} \lambda^{10}_{1B-L} - \lambda^{10}_{1R} = \sum_i a_i \eta_i \\ \lambda^{10}_{1R} - \lambda^{10}_{2\mathrm{L}} = \sum_i b_i \eta_i \\ \lambda^{10}_{2\mathrm{L}} - \lambda^{10}_{3\mathrm{C}} = \sum_i c_i \eta_i \end{cases}, \tag{5.1}$$

where the coefficients a_i, b_i, and c_i are given in Eq. (4.11). Also, for simplicity, we have chosen to label η_i with $i = 1, \ldots, 65$. In this system there are 65 unknown variables, and only three equations. One particular solution is of interest, which is the one that minimizes the Euclidean norm of the vector

$$\boldsymbol{\eta} = \begin{bmatrix} \eta_1 \ldots \eta_{65} \end{bmatrix}^T, \tag{5.2}$$

which contains all of the different η_i at M_{GUT}. This solution is interesting since having lower values of these parameters makes the model more viable. If we create the 3×65 matrix

$$A = \begin{bmatrix} a_1 \ldots a_{65} \\ b_1 \ldots b_{65} \\ c_1 \ldots c_{65} \end{bmatrix}, \tag{5.3}$$

and the vector

$$\boldsymbol{y} = \left[\lambda^{10}_{1B-L} - \lambda^{10}_{1R} \quad \lambda^{10}_{1R} - \lambda^{10}_{2\mathrm{L}} \quad \lambda^{10}_{2\mathrm{L}} - \lambda^{10}_{3\mathrm{C}}\right]^T , \tag{5.4}$$

the system can be written as

$$A\boldsymbol{\eta} = \boldsymbol{y} . \tag{5.5}$$

The solution with the smallest norm can then be found as the least-squares solution

$$\boldsymbol{\eta} = \left(A^T A\right)^{-1} A^T \boldsymbol{y} , \tag{5.6}$$

as long as the matrix inverse $(A^T A)^{-1}$ exists. If it does not, a singular value decomposition can be used instead. Either way, both of these cases are included in the `lstsq` solver in the `NumPy` package [66]. The maximum value $\eta_{\max}$ in this vector of η_i, i.e. $\eta_{\max} = \max_{1\leq i\leq 65}(\eta_i)$, can then be used as a measure of what is needed to give the required threshold corrections.

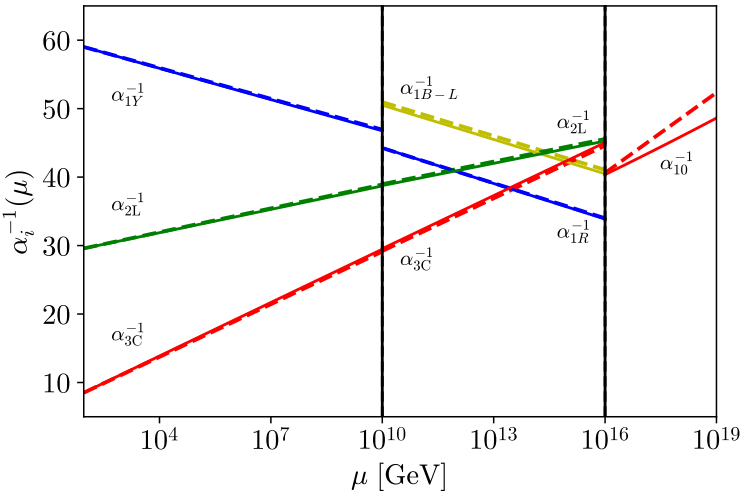

Figure 5.4: An example of unification, allowed by threshold corrections, in the model with $\mathcal{G}_{3211}$ as the intermediate symmetry. The running of the coupling constants in $\mathcal{G}_{\mathrm{SM}}$, $\mathcal{G}_{3211}$, and SO(10) are shown to one-loop order (dashed) and two-loop order (solid). Here, the scales are chosen as $M_{\mathrm{I}} = 10^{10}$ GeV and $M_{\mathrm{GUT}} = 10^{16}$ GeV, and are shown as vertical lines. The threshold corrections are then found following the described procedure. Minimization with respect to x is done, giving $\eta_{\max} = 4.28$ for $x = 1.15$ in the one-loop case, and $\eta_{\max} = 4.26$ for $x = 1.14$ in the two-loop case.

As a final step, the dependence on the parameter x can then be removed, by minimizing $\eta_{\max}$ with respect to x for each combination of M_{I} and M_{GUT}. This parameter has no particular physical importance, as it is just something that was

inserted in order to invert the system. Such a minimization then just ensures that we have the solution giving the lowest value of $\eta_{\max}$. The minimization is done using the `minimize` function from the `SciPy` package, using a Nelder–Mead algorithm. Figure 5.4 shows an example of the running in the model, when it is solved in this way. The scales are chosen as $M_{\mathrm{I}} = 10^{10}\,\mathrm{GeV}$ and $M_{\mathrm{GUT}} = 10^{16}\,\mathrm{GeV}$, while x and $\boldsymbol{\eta}$ are found from the solver.

Using this algorithm, we can also create a grid of different combinations of M_{I} and M_{GUT}, to see how the required threshold corrections change. The resulting values of $\eta_{\max}$, for different scales, are shown in figure 5.5. In both plots, the color scale shows how the value of this largest η_i changes over the grid. There are also contour lines showing some different values of $\eta_{\max}$, as well as the limit given by the proton lifetime. Here, the region $M_{\mathrm{I}} > M_{\mathrm{GUT}}$ is not plotted at all, since it now is possible to completely choose the scales.

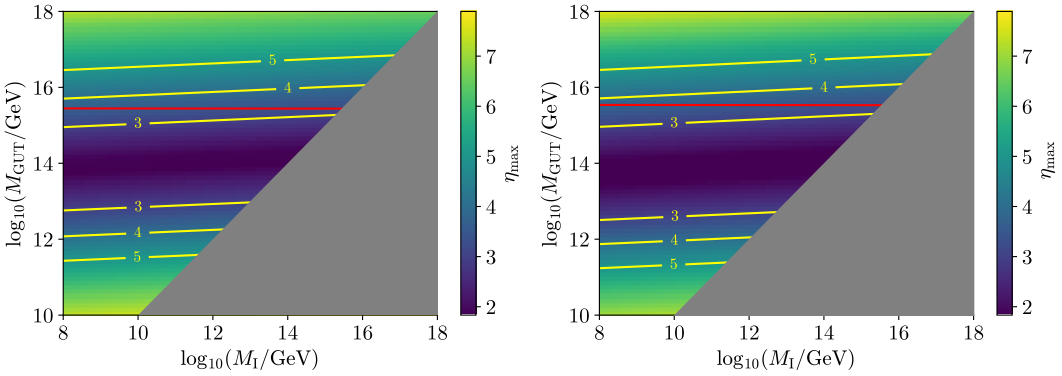

(a) One-loop order **(b)** Two-loop order

Figure 5.5: The maximum value $\eta_{\max}$ that is needed to achieve unification in the model with $\mathcal{G}_{3211}$ (without kinetic mixing effects) as the intermediate symmetry, for different combinations of M_{I} and M_{GUT}. Also, the value at each point in the grid is minimized individually with respect to the parameter x. Some particular values of $\eta_{\max}$ in the color scale are shown by the yellow contour lines, and the red line is the limit required for suppressing proton decay, excluding all points under it. Finally, the grey section is the unphysical region where $M_{\mathrm{I}} > M_{\mathrm{GUT}}$.

We can in both of these plots note that there is very little dependence on where the intermediate scale M_{I} is placed, as compared to how much $\eta_{\max}$ changes when M_{GUT} changes. This peculiarity is also a consequence of the fact that the intermediate symmetry is so similar to the SM, since it results in the β-function coefficients for the two groups being almost the same. As we saw in the previous plots, this results in the slopes for the coupling constants being almost the same above and below M_{I}. Therefore, changing M_{I} barely has an effect on where the couplings end up at M_{GUT}, or, more importantly, how much they are separated.

On the other hand, changing M_{GUT} has a large impact on the separation of the couplings, and thus on the size of the threshold corrections that are needed.

5.2.1 Kinetic mixing

When adding the effects of kinetic mixing to the model, a similar numerical procedure can be used to generate results. The only difference, apart from the changes to β-functions and matching conditions, is that now there are two parameters of no physical relevance, x and y. We can solve the system of equations for $\eta_{\max}$ just as explained in the last section, now giving M_{I}, M_{GUT}, x, and y as input. However, we must also consider the condition $\tilde{g}(M_{\mathrm{GUT}}) = 0$, which makes some combinations of the parameters x and y impossible for certain scales. We can then again minimize $\eta_{\max}$ for each combination of M_{I} and M_{GUT}, but now with respect to both x and y. An example of such a solution is plotted in figure 5.6, similarly to the one in figure 5.4.

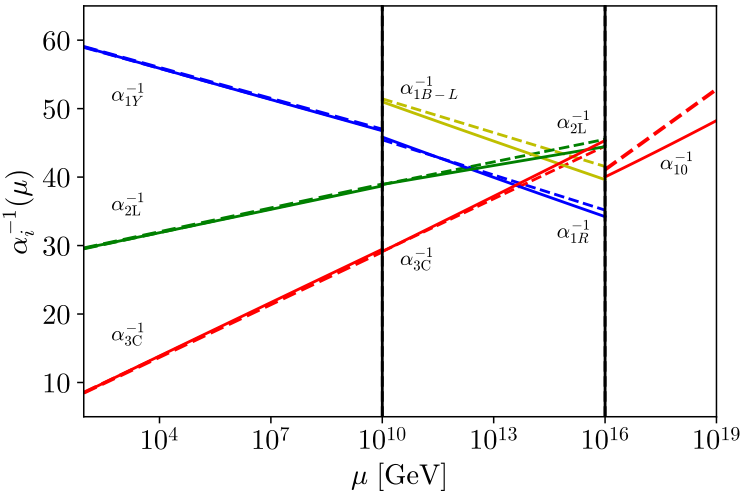

Figure 5.6: An example of unification, allowed by threshold corrections, in the model with $\mathcal{G}_{3211}$ as the intermediate symmetry, including the effects of kinetic mixing. The running of the coupling constants in $\mathcal{G}_{\mathrm{SM}}$, $\mathcal{G}_{3211}$, and SO(10) are shown to one-loop order (dashed) and two-loop order (solid). Here, the scales are chosen as $M_{\mathrm{I}} = 10^{10}\,\mathrm{GeV}$ and $M_{\mathrm{GUT}} = 10^{16}\,\mathrm{GeV}$, and are shown as vertical lines. The threshold corrections are then found following the described procedure. Minimization with respect to x and y is done, giving $\eta_{\max} = 3.81$ for $x = 1.13$ and $y = 0.02$ in the one-loop case, and $\eta_{\max} = 3.91$ for $x = 1.11$ and $y = 0.02$ in the two-loop case.

Apart from the optimal value of x changing slightly, we can also note the qualitative difference that the slopes of the two-loop couplings now change noticeably.

We can again create a grid of scales M_{I} and M_{GUT}, and solve for $\eta_{\max}$ for each point, minimized with respect to x and y. The resulting values are shown in figure 5.7. Qualitatively, we see there that the situation was improved by the addition of kinetic mixing, as expected by the earlier plot. Improved means that we require smaller values of $\eta_{\max}$ to reach the same scales, compared to the case without mixing effects. The most striking differences seem to be at combinations where the value of M_{I} is low and the value of M_{GUT} is high. This may be due to the difference in slopes at two-loop order noted earlier, as it then gets enough space between the two scales to make a significant impact on where the couplings are at the unification scale M_{GUT}.

The difference coming from kinetic mixing effects can also be quantified. If we by $\eta^0_{\max}$ denote the values without kinetic mixing, we can define the relative difference

$$\Delta\eta \equiv \frac{\eta^0_{\max} - \eta_{\max}}{\eta^0_{\max}} \,. \tag{5.7}$$

By combining the values seen in figures 5.5 and 5.7, we can then plot how this difference changes depending on the scales M_{I} and M_{GUT}. This is showed in figure 5.8. It can be seen that the addition of kinetic mixing effects can decrease the required maximum value of η_i by around 20 percent in some places. The difference is also sometimes negative, but mostly in regions that are unphysical anyway.

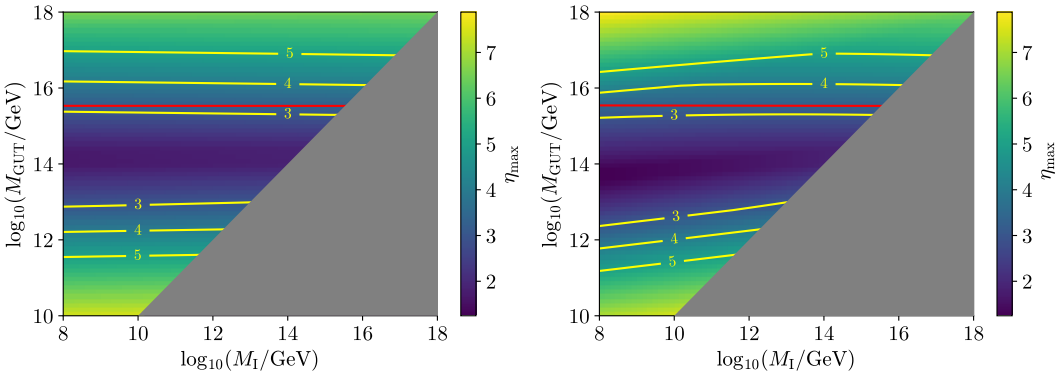

(a) One-loop order

(b) Two-loop order

Figure 5.7: The color scale shows the maximum value $\eta_{\max}$ that is needed to achieve unification in the model with $\mathcal{G}_{3211}$ (including kinetic mixing effects) as the intermediate symmetry, for different combinations of M_{I} and M_{GUT}. Also, the value at each point in the grid is minimized individually with respect to the parameters x and y. Some particular values of $\eta_{\max}$ are shown by the yellow contour lines, and the red line is the limit required for suppressing proton decay, excluding all points under it. Finally, the grey section is the unphysical region where $M_{\mathrm{I}} > M_{\mathrm{GUT}}$.

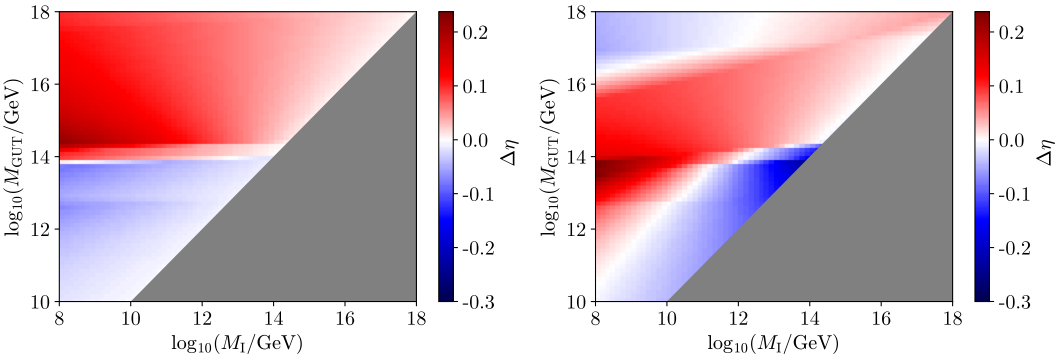

(a) One-loop order **(b)** Two-loop order

Figure 5.8: The relative difference $\Delta\eta$ between values of $\eta_{\max}$ computed in models with $\mathcal{G}_{3211}$ as the intermediate symmetry, with and without kinetic mixing. The individual values for both models are shown in figures 5.5 and 5.7, and the resulting differences are shown here.

Chapter 6

Summary and conclusions

First, in Ch. 2, we discussed the relevant background theory for this thesis. We started with the gauge symmetries of QFTs, which is the very foundation of the models that are analyzed here. After that, the SM was introduced, which is the currently used theory of particle physics that models must agree with at lower energies. This was followed by a discussion on renormalization group running and GUTs, where specifically SO(10) was mentioned as a promising candidate for a GUT gauge group. Also, the effects of kinetic mixing were mentioned, threshold effects were introduced, and finally, the possible decays of protons in theories beyond the SM were discussed.

In Ch. 3, the two different models analyzed in this thesis were discussed. The first one, model 1, has $\mathcal{G}_{51}$ as an intermediate symmetry between SO(10) and the SM, while the second one, model 2, has $\mathcal{G}_{3211}$ as the intermediate symmetry. The particle content and charge normalization in the models were also discussed, and it was explained why it is not possible to achieve unification at tree-level matching in either of the two models. This explanation differs a bit between the two models, so their individual characteristics were also brought up.

Then, in Ch. 4, threshold effects were computed for the two models, which result in corrections that affect the matching conditions where the symmetry breaking occurs. These corrections can then allow us to achieve unification in our two models. It was examined how different fields can be placed at different scales in the two models, and how these fields affect the expressions for the corrections. It was then shown how these corrections alter the equations from the previous chapter.

Finally, in Ch. 5, the numerical procedure was explained, and the corresponding results were shown. The equations from the previous chapters, including threshold corrections, were then solved numerically, in order to find the scales for unification. As the two models have different characteristics, the approach for this numerical analysis was different for each model, as explained in detail.

The main purpose of this thesis has been to examine the viability of two different models based on SO(10) as a GUT gauge group, with different intermediate

symmetries. It was shown that unification indeed is possible in both models, with sufficiently large threshold corrections. The follow-up question is then whether or not these corrections are small enough for the models to be considered viable. We could impose a limit for acceptable solutions, when fields contributing to threshold effects have masses one order of magnitude from the symmetry breaking scale. The models can then be considered viable, although close to the limit. As part of this thesis, it was also examined how much of a difference it makes to add the effects of kinetic mixing in model 2, as compared to when they are neglected. It could be noted that kinetic mixing effects made a small but notable impact on how easy it was to achieve unification in that model.

GUTs are a fascinating way of extending theories of particle physics beyond the SM, and SO(10) in particular is a fitting candidate for the corresponding gauge group. The results seen here might be important lessons to keep in mind when building GUT models in general, where similar issues can arise. Models are not necessarily rendered useless just based on that unification is not possible at tree-level matching, and taking into account kinetic mixing effects can be helpful in achieving unification.

Bibliography

[1] CMS, S. Chatrchyan *et al.*, *Observation of a new boson at a mass of 125 GeV with the CMS Experiment at the LHC*, Phys. Lett. B **716**, 30 (2012), 1207.7235.

[2] ATLAS, G. Aad *et al.*, *Observation of a new particle in the search for the Standard Model Higgs boson with the ATLAS detector at the LHC*, Phys. Lett. B **716**, 1 (2012), 1207.7214.

[3] Super-Kamiokande, Y. Fukuda *et al.*, *Neutrino induced upward stopping muons in Super-Kamiokande*, Phys. Lett. B **467**, 185 (1999), hep-ex/9908049.

[4] G. Lazarides, Q. Shafi and C. Wetterich, *Proton Lifetime and Fermion Masses in an SO(10) Model*, Nucl. Phys. B **181**, 287 (1981).

[5] H. Georgi and S. Glashow, *Unity of All Elementary Particle Forces*, Phys. Rev. Lett. **32**, 438 (1974).

[6] A. Buras *et al.*, *Aspects of the Grand Unification of Strong, Weak and Electromagnetic Interactions*, Nucl. Phys. B **135**, 66 (1978).

[7] M. E. Peskin and D. V. Schroeder, *An Introduction to quantum field theory,* (Addison-Wesley, Reading, USA, 1995).

[8] H. Georgi, *Lie Algebras in Particle Physics: From Isospin to Unified Theories* (Avalon Publishing, 1999).

[9] C. N. Yang and R. L. Mills, *Conservation of Isotopic Spin and Isotopic Gauge Invariance*, Phys. Rev. **96**, 191 (1954).

[10] S. Weinberg, *A Model of Leptons*, Phys. Rev. Lett. **19**, 1264 (1967).

[11] A. Salam and J. C. Ward, *Weak and electromagnetic interactions*, Nuovo Cim. **11**, 568 (1959).

[12] S. L. Glashow, *The renormalizability of vector meson interactions*, Nucl. Phys. **10**, 107 (1959).

[13] D. J. Gross and F. Wilczek, *Ultraviolet Behavior of Nonabelian Gauge Theories*, Phys. Rev. Lett. **30**, 1343 (1973).

[14] H. Politzer, *Reliable Perturbative Results for Strong Interactions?*, Phys. Rev. Lett. **30**, 1346 (1973).

[15] P. W. Anderson, *Plasmons, Gauge Invariance, and Mass*, Phys. Rev. **130**, 439 (1963).

[16] P. W. Higgs, *Broken Symmetries and the Masses of Gauge Bosons*, Phys. Rev. Lett. **13**, 508 (1964).

[17] F. Englert and R. Brout, *Broken Symmetry and the Mass of Gauge Vector Mesons*, Phys. Rev. Lett. **13**, 321 (1964).

[18] G. Guralnik, C. Hagen and T. Kibble, *Global Conservation Laws and Massless Particles*, Phys. Rev. Lett. **13**, 585 (1964).

[19] C. Bollini and J. Giambiagi, *Dimensional Renormalization: The Number of Dimensions as a Regularizing Parameter*, Nuovo Cim. B **12**, 20 (1972).

[20] G. 't Hooft and M. Veltman, *Regularization and Renormalization of Gauge Fields*, Nucl. Phys. B **44**, 189 (1972).

[21] W. Pauli and F. Villars, *On the Invariant Regularization in Relativistic Quantum Theory*, Rev. Mod. Phys. **21**, 434 (1949).

[22] G. 't Hooft, *Dimensional regularization and the renormalization group*, Nucl. Phys. B **61**, 455 (1973).

[23] S. Weinberg, *New approach to the renormalization group*, Phys. Rev. D **8**, 3497 (1973).

[24] B. Holdom, *Two* U(1)*'s and Epsilon Charge Shifts*, Phys. Lett. B **166**, 196 (1986).

[25] D. Jones, *Two-loop β function for a $G_1 \times G_2$ gauge theory*, Phys. Rev. D **25**, 581 (1982).

[26] I. Jack and H. Osborn, *General Two Loop Beta Functions for Gauge Theories With Arbitrary Scalar Fields*, J. Phys. A **16**, 1101 (1983).

[27] M. E. Machacek and M. T. Vaughn, *Two Loop Renormalization Group Equations in a General Quantum Field Theory. 1. Wave Function Renormalization*, Nucl. Phys. B **222**, 83 (1983).

[28] M. E. Machacek and M. T. Vaughn, *Two Loop Renormalization Group Equations in a General Quantum Field Theory. 2. Yukawa Couplings*, Nucl. Phys. B **236**, 221 (1984).

[29] M. E. Machacek and M. T. Vaughn, *Two Loop Renormalization Group Equations in a General Quantum Field Theory. 3. Scalar Quartic Couplings*, Nucl. Phys. B **249**, 70 (1985).

[30] D. Meloni, T. Ohlsson and M. Pernow, *Threshold effects in* SO(10) *models with one intermediate breaking scale*, (2019), 1911.11411.

[31] Particle Data Group, M. Tanabashi *et al.*, *Review of Particle Physics*, Phys. Rev. D **98**, 030001 (2018).

[32] T. P. Cheng and L. F. Li, *Gauge theory of elementary particle physics* (Oxford University Press, 1984).

[33] H. Fritzsch and P. Minkowski, *Unified Interactions of Leptons and Hadrons*, Annals Phys. **93**, 193 (1975).

[34] H. Georgi, *Unified Gauge Theories*, Stud. Nat. Sci. **9**, 329 (1975).

[35] H. Georgi, *The State of the Art—Gauge Theories*, AIP Conf. Proc. **23**, 575 (1975).

[36] G. Altarelli and D. Meloni, *A non supersymmetric* SO(10) *grand unified model for all the physics below* $M_{\rm GUT}$, JHEP **08**, 021 (2013), 1305.1001.

[37] M. Pernow, *Phenomenology of* SO(10) *Grand Unified Theories*, Licentiate thesis, KTH, School of Engineering Sciences (SCI), Physics, Particle and Astroparticle Physics, 2019.

[38] H. Georgi, H. R. Quinn and S. Weinberg, *Hierarchy of Interactions in Unified Gauge Theories*, Phys. Rev. Lett. **33**, 451 (1974).

[39] B. Brahmachari and A. Raychaudhuri, *Kinetic mixing and symmetry breaking dependent interactions of the dark photon*, Nucl. Phys. B **887**, 441 (2014), 1409.2082.

[40] S. Bertolini, L. Di Luzio and M. Malinský, *Light color octet scalars in the minimal* SO(10) *grand unification*, Phys. Rev. D **87**, 085020 (2013), 1302.3401.

[41] H. M. Tran, *Kinetic mixing in models with an extra Abelian gauge symmetry*, Communications in Physics **28**, 41 (2018).

[42] J. Ellis, *TikZ-Feynman: Feynman diagrams with TikZ*, Comput. Phys. Commun. **210**, 103 (2017), 1601.05437.

[43] M. X. Luo and Y. Xiao, *Renormalization group equations in gauge theories with multiple* U(1) *groups*, Phys. Lett. B **555**, 279 (2003), hep-ph/0212152.

[44] S. Bertolini, L. Di Luzio and M. Malinský, *Intermediate mass scales in the non-supersymmetric* SO(10) *grand unification: A reappraisal*, Phys. Rev. D **80**, 015013 (2009), 0903.4049.

[45] L. J. Hall, *Grand Unification of Effective Gauge Theories*, Nucl. Phys. B **178**, 75 (1981).

[46] B. A. Ovrut and H. J. Schnitzer, *Gauge Theory and Effective Lagrangian*, Nucl. Phys. B **189**, 509 (1981).

[47] S. Weinberg, *Effective Gauge Theories*, Phys. Lett. B **91**, 51 (1980).

[48] R. M. Fonseca, M. Malinský and F. Staub, *Renormalization group equations and matching in a general quantum field theory with kinetic mixing*, Phys. Lett. B **726**, 882 (2013), 1308.1674.

[49] Super-Kamiokande, K. Abe *et al.*, *Search for proton decay via* $p \to \nu K^+$ *using 260 kiloton* $\cdot$ *year data of Super-Kamiokande*, Phys. Rev. D **90**, 072005 (2014), 1408.1195.

[50] Super-Kamiokande, K. Abe *et al.*, *Search for proton decay via* $p \to e^+\pi^0$ *and* $p \to \mu^+\pi^0$ *in 0.31 megaton* $\cdot$ *years exposure of the Super-Kamiokande water Cherenkov detector*, Phys. Rev. D **95**, 012004 (2017), 1610.03597.

[51] K. Babu, J. C. Pati and Z. Tavartkiladze, *Constraining Proton Lifetime in* SO(10) *with Stabilized Doublet-Triplet Splitting*, JHEP **06**, 084 (2010), 1003.2625.

[52] P. Nath and P. Fileviez Perez, *Proton stability in grand unified theories, in strings and in branes*, Phys. Rept. **441**, 191 (2007), hep-ph/0601023.

[53] S. Dimopoulos and H. Georgi, *Extended Survival Hypothesis and Fermion Masses*, Phys. Lett. B **140**, 67 (1984).

[54] S. M. Barr, *A New Symmetry Breaking Pattern for* SO(10) *and Proton Decay*, Phys. Lett. B **112**, 219 (1982).

[55] J. R. Ellis *et al.*, *Aspects of the Flipped Unification of Strong, Weak and Electromagnetic Interactions*, Nucl. Phys. B **311**, 1 (1988).

[56] J. Derendinger, J. E. Kim and D. V. Nanopoulos, *Anti-*SU(5), Phys. Lett. B **139**, 170 (1984).

[57] M. Parida and C. Hazra, *Superheavy-Higgs-scalar effects in effective gauge theories from* SO(10) *grand unification with low-mass right-handed gauge bosons*, Phys. Rev. D **40**, 3074 (1989).

[58] M. Parida, P. Patra and C. Hazra, *Models with natural seesaw mechanism for neutrino masses with identical parity and* $\mathrm{SU(2)_R}$ *breaking scales*, Phys. Rev. D **43**, 2351 (1991).

[59] F. Lyonnet, *Impact of kinetic mixing in beta functions at two-loop*, Phys. Rev. D **94**, 076008 (2016), 1608.07271.

[60] F. Lyonnet and I. Schienbein, *PyR@TE 2: A Python tool for computing RGEs at two-loop*, Comput. Phys. Commun. **213**, 181 (2017), 1608.07274.

[61] F. Lyonnet *et al.*, *PyR@TE: Renormalization Group Equations for General Gauge Theories*, Comput. Phys. Commun. **185**, 1130 (2014), 1309.7030.

[62] F. del Aguila, G. Coughlan and M. Quiros, *Gauge coupling renormalization with several* U(1) *factors*, Nucl. Phys. B **307**, 633 (1988), [Erratum: Nucl. Phys. B **312**, 751 (1989)].

[63] T. G. Rizzo, *Gauge kinetic mixing and leptophobic* Z′ *in* E(6) *and* SO(10), Phys. Rev. D **59**, 015020 (1998), hep-ph/9806397.

[64] R. Slansky, *Group Theory for Unified Model Building*, Phys. Rept. **79**, 1 (1981).

[65] P. Virtanen *et al.*, *SciPy 1.0–Fundamental Algorithms for Scientific Computing in Python*, Nature Meth. **17**, 261 (2020), 1907.10121.

[66] T. E. Oliphant, *A guide to NumPy*, Vol. 1 (Trelgol Publishing USA, 2006).